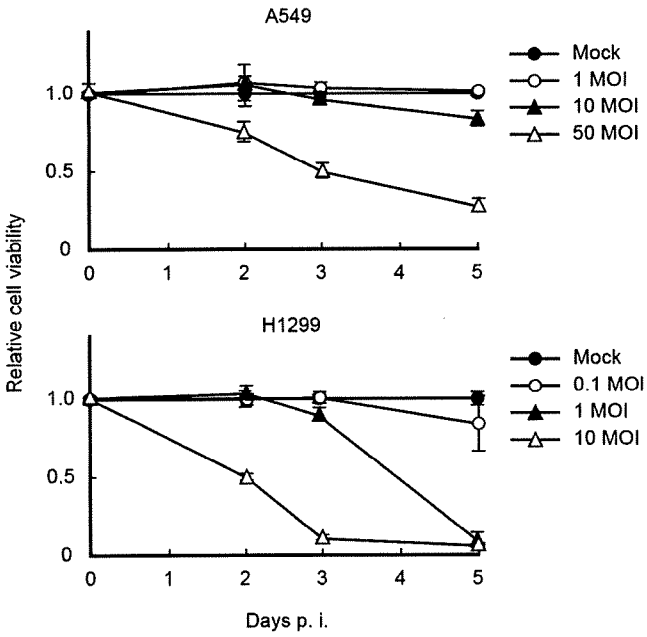

Fig. 1 Cytopathic effects of OBP-301 on H1299 and A549 lung cancer cell lines *in vitro*. Each cell was infected with OBP-301 at the indicated MOI and cell viability was evaluated by XTT assay (no virus=1.0). Data are mean±SD values

Introduction) and OBP-401, a modified OBP-301 that contains the GFP gene [12] (data not shown).

Inhibitory effects of CDV on viral replication of OBP-301

Finally, we examined whether CDV inhibits the replication of OBP-301 *in vitro*. We previously used two methods to quantify viral replication, biological plaque forming assay using 293 cells [7] and real-time PCR assay targeting adenoviral E1A sequence [8, 9], and found that both assays could detect viral replication similarly. H1299 cells were infected with OBP-301 or wt-Ad, followed by treatment with CDV. Wt-Ad was used for positive control in this assay since it had been reported that CDV had antiviral activity against wt-Ad. To measure the viral DNA, we quantified E1A copy number of cells infected with OBP-301 or wt-Ad by real-time PCR assay. CDV reduced the relative E1A copy number in both wt-Ad and OBP-301-infected cells and the effect was concentration-dependent, indicating that CDV inhibited viral replication of OBP-301 and wt-Ad in H1299 cells (Fig. 3). The calculated EC_{50} (E1A) value for OBP-301 was 19.55 μM.

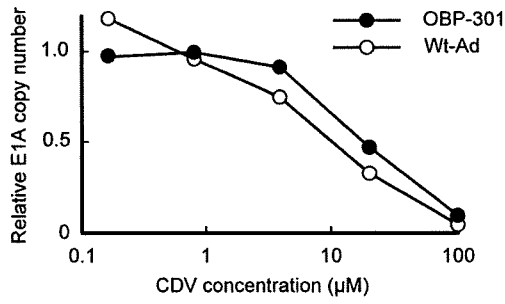

Fig. 3 Inhibition of OBP-301 replication in H1299 cells by CDV. Cells were infected with OBP-301 or wild-type AdV at MOI of 10, followed by the addition of CDV at the indicated concentrations. Cells were collected after 24 hours infection, total DNA was extracted, and viral E1A copy number was determined by quantitative real-time PCR analysis (with virus/no CDV=1.0)

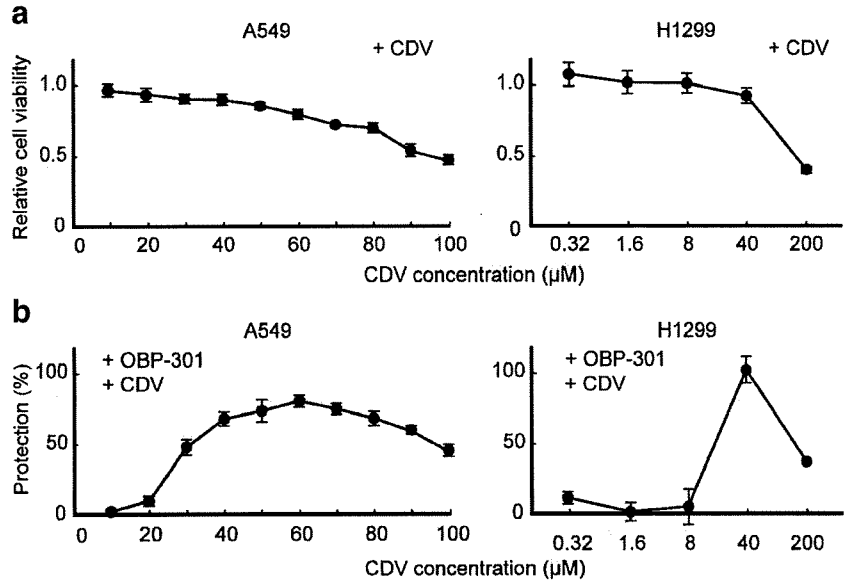

Fig. 2 Inhibition of cytopathic effects of OBP-301 by CDV in human lung cancer cell lines. (**a**) Cells were treated with CDV at the indicated concentrations and incubated for 7 days. The relative cell viability was evaluated by XTT assay. Data are mean±SD values. (**b**) Cells were infected with OBP-301 (1 MOI in H1299 and 5 MOI in A549, PFU/cell), followed by the addition of CDV at the indicated concentrations. Protection was calculated as described in "Material and methods". Data are mean±SD values

Discussion

OBP-301 has been developed as an oncolytic viral agent for the treatment of human cancer and is currently used in a phase-I clinical trial. Although replication of OBP-301 is limited in normal cells evaluated *in vitro* and *in vivo* mouse model, the effect of OBP-301 in human is still unknown. In the phase-II clinical trial of ONYX-015, an E1B-55 kDa-deleted adenovirus mutant, adenoviral viremia occurred even in the presence of neutralizing antibodies and antiviral cytokines [13]. Several antiviral drugs are used for other DNA viruses, e.g. aciclovir, a synthetic acyclic purine-nucleoside analogue, for Herpes simplex virus (HSV) [14], and ganciclovir (GCV) for Cytomegalovirus infections [15]. For AdV infections, it has been reported that CDV exhibits potent inhibitory effects against several adenoviral serotypes in cell culture models [10, 16]. We considered that CDV can be used as antiviral drug for OBP-301.

The purpose of using CDV clinically is to avoid toxic effects of OBP-301 in normal tissues, when viral replication becomes uncontrollable. However, it is difficult to examine the inhibitory effect of CDV on cytopathic effect of OBP-301 in normal cells, because OBP-301 replicates and lyses only in cancer cells [7–9]. Therefore, we used human cancer cell lines to assess the potential antiviral activity of CDV. We showed that the cytopathic effects of OBP-301 were efficiently suppressed by CDV treatment at concentrations that did not affect cell growth (Fig. 2). Despite the high susceptibility of H1299 cells to OBP-301 infection (Fig. 1), CDV inhibited the cytopathic effects of OBP-301, suggesting that CDV has potent antiviral activity against OBP-301. The 50% effective concentration of CDV in A549 cells was in agreement with the published data using human wt-Ad [17], indicating that the inhibitory activity against the cytopathic effect of OBP-301 was equivalent to that of wt-Ad.

The mechanism of the antiviral effect of CDV is that of inhibition of viral replication by targeting the viral DNA polymerase [18]. The anti-adenoviral effect of CDV is quantified by evaluating the viral progeny in adenovirus-infected cells using quantitative PCR analysis [16]. We demonstrated that the replication of OBP-301 was inhibited by CDV in a concentration-dependent manner (Fig. 3). In addition, the 50% effective concentration on viral DNA copy number was almost the same as the 50% effective concentration on cell death by OBP-301 infection, suggesting that CDV inhibited the cytopathic effect of OBP-301 by inhibiting the replication of OBP-301. Recently, antiviral effect of CDV against wt-Ad in immunosuppressed Syrian hamster model was reported [19]. The 50% inhibitory concentration of CDV on viral DNA copy number in OBP-301 was slightly higher than that of wt-Ad (Fig. 3). Differences at E1A region between OBP-301 and wt-Ad may affect of CDV activity on viral replication. It has been reported that CDV-resistant human Ad mutants were isolated by continuous passage *in vitro* condition [20]. Quality assurance and quality control of the master virus bank have been intensively performed for OBP-301 used in the current clinical trials; emergence of CDV-resistant OBP-301 variant, however, should be considered and long-term susceptibility of CDV against OBP-301 will be studied in the future clinical trials.

In conclusion, our *in vitro* data indicate that CDV can effectively inhibit the oncolytic activity of OBP-301 by inhibiting the replication of OBP-301. CDV may be a potential antiviral agent for OBP-301 in clinical trial.

References

1. Kirn D, Martuza RL, Zwiebel J (2001) Replication-selective virotherapy for cancer: biological principles, risk management and future directions. Nat Med 7:781–787. doi:10.1038/89901
2. Kirn D (2000) Replication-selective oncolytic adenoviruses: virotherapy aimed at genetic targets in cancer. Oncogene 19:6660–6669. doi:10.1038/sj.onc.1204094
3. Chu RL, Post DE, Khuri FR, Van Meir EG (2004) Use of replicating oncolytic adenoviruses in combination therapy for cancer. Clin Cancer Res 10:5299–5312. doi:10.1158/1078-0432.CCR-0349-03
4. Davis JJ, Fang B (2005) Oncolytic virotherapy for cancer treatment: challenges and solutions. J Gene Med 7:1380–1389. doi:10.1002/jgm.800
5. Nakamura TM, Morfin GB, Chapman KB, Weinrich SL, Andrews WH, Lingner J et al (1997) Telomerase catalytic subunit homologs from fission yeast and human. Science 277:955–959. doi:10.1126/science.277.5328.955
6. Kim NW, Piatyszek MA, Prowse KR, Harley CB, West MD, Ho PL et al (1994) Specific association of human telomerase activity with immortal cells and cancer. Science 266:2011–2015. doi:10.1126/science.7605428
7. Kawashima T, Kagawa S, Kobayashi N, Shirakiya Y, Umeoka T, Teraishi F et al (2004) Telomerase-specific replication-selective virotherapy for human cancer. Clin Cancer Res 10:285–292. doi:10.1158/1078-0432.CCR-1075-3
8. Taki M, Kagawa S, Nishizaki M, Mizuguchi H, Hayakawa T, Kyo S et al (2005) Enhanced oncolysis by a tropism-modified telomerase-specific replication-selective adenoviral agent OBP-405 (Telomelysin-RGD). Oncogene 24:3130–3140. doi:10.1038/sj.onc.1208460
9. Hashimoto Y, Watanabe Y, Shirakiya Y, Uno F, Kagawa S, Kawamura H et al (2008) Establishment of biological and pharmacokinetic assays of telomerase-specific replication-selective adenovirus. Cancer Sci 99:385–390. doi:10.1111/j.1349-7006.2007.00665.x
10. Gordon YJ, Romanowski E, Araullo-Cruz T, Seaberg L, Erzurum S, Tolman R et al (1991) Inhibitory effect of (S)-HPMPC, (S)-HPMPA, and 2'¢-nor-cyclic GMP on clinical ocular adenoviral isolates is serotype-dependent in vitro. Antivir Res 16:11–16. doi:10.1016/0166-3542(91)90054-U
11. De Clercq E (2003) Clinical potential of the acyclic nucleoside phosphonates cidofovir, adefovir, and tenofovir in treatment of DNA virus and retrovirus infections. Clin Microbiol Rev 16:569–596. doi:10.1128/CMR.16.4.569-596.2003

12. Kishimoto H, Kojima T, Watanabe Y, Kagawa S, Fujiwara T, Uno F et al (2006) *In vivo* imaging of lymph node metastasis with telomerase-specific replication-selective adenovirus. Nat Med 12:1213–1219. doi:10.1038/nm1404
13. Reid T, Galanis E, Abbruzzese J, Sze D, Wein LM, Andrews J et al (2002) Hepatic arterial infusion of a replication-selective oncolytic adenovirus (dl1520): phase II viral, immunologic, and clinical endpoints. Cancer Res 62:6070–6079
14. Whitley RJ, Roizman B (2001) Herpes simplex virus infection. Lancet 357:1513–1518. doi:10.1016/S0140-6736(00)04638-9
15. Biron KK (2006) Antiviral drugs for cytomegalovirus diseases. Antivir Res 71:154–163. doi:10.1016/j.antiviral.2006.05.002
16. Naesens L, Lenaerts L, Andrei G, Snoeck R, Van Beers D, Holy A et al (2005) Antiadenovirus activities of several classes of nucleoside and nucleotide analogues. Antimicrob Agents Chemother 49:1010–1016. doi:10.1128/AAC.49.3.1010-1016.2005
17. Morfin F, Dupuis-Girod S, Mundweiler S, Falcon D, Carrington D, Sedlacek P et al (2005) *In vitro* susceptibility of adenovirus to antiviral drugs is species-dependent. Antivir Ther 10:225–229
18. Kinchington PR, Araullo-Cruz T, Vergnes JP, Yates K, Gordon YJ (2002) Sequence changes in the human adenovirus type 5 DNA polymerase associated with resistance to the broad spectrum antiviral cidofovir. Antivir Res 56:73–84. doi:10.1016/S0166-3542(02)00098-0
19. Toth K, Spencer JF, Dhar D, Sagartz JE, Buller RM, Painter GR et al (2008) Hexadecyloxypropyl-cidofovir, CMX001, prevents adenovirus-induced mortality in a permissive, immunosuppressed animal model. Proc Natl Acad Sci U S A 105:7293–7297. doi:10.1073/pnas.0800200105
20. Gordon YJ, Araullo-Cruz TP, Johnson YF, Romanowski EG, Kinchington PR (1996) Isolation of human adenovirus type 5 variants resistant to the antiviral cidofovir. Invest Ophthalmol Vis Sci 37:2774–2778

Preclinical evaluation of synergistic effect of telomerase-specific oncolytic virotherapy and gemcitabine for human lung cancer

Dong Liu,[1,3] Toru Kojima,[1,2] Masaaki Ouchi,[4] Shinji Kuroda,[1,2] Yuichi Watanabe,[2,4] Yuuri Hashimoto,[2,4] Hideki Onimatsu,[4] Yasuo Urata,[4] and Toshiyoshi Fujiwara[1,2]

[1]Center for Gene and Cell Therapy, Okayama University Hospital; [2]Division of Surgical Oncology, Department of Surgery, Okayama University Graduate School of Medicine, Dentistry and Pharmaceutical Sciences, Okayama, Japan; [3]Research Center of Lung Cancer, Shanghai Pulmonary Hospital, The Tongji University, Shanghai, China; and [4]Oncolys BioPharma, Inc., Tokyo, Japan

Abstract

A phase I dose-escalation study of telomerase-specific oncolytic adenovirus, OBP-301 (Telomelysin), is now under way in the United States to assess feasibility and to characterize its pharmacokinetics in patients with advanced solid tumors. The present preclinical study investigates whether OBP-301 and a chemotherapeutic agent that is commonly used for lung cancer treatment, gemcitabine, are able to enhance antitumor effects *in vitro* and *in vivo*. The antitumor effects of OBP-301 infection and gemcitabine were evaluated by 2,3-bis[2-methoxy-4-nitro-5-sulfophenyl]-2H-tetrazolium-5-carboxanilide inner salt assay. *In vivo* antitumor effects of intratumoral injection of OBP-301 in combination with systemic administration of gemcitabine were assessed on *nu/nu* mice s.c. xenografted with human lung tumors. OBP-301 infection combined with gemcitabine resulted in very potent synergistic cytotoxicity in human lung cancer cells. The three human lung cancer cell lines treated with OBP-301 for 24 hours tended to accumulate in S phase compared with controls. The proportion of cells in S phase increased from 43.85% to 56.41% in H460 cells, from 46.72% to 67.09% in H322 cells, and from 38.22% to 57.67% in H358 cells. Intratumoral injection of OBP-301 combined with systemic administration of gemcitabine showed therapeutic synergism in human lung tumor xenografts. Our data suggest that the combination of OBP-301 and gemcitabine enhances the antitumor effects against human lung cancer. We also found that the synergistic mechanism may be due to OBP-301–mediated cell cycle accumulation in S phase. These results have important implications for the treatment of human lung cancer. [Mol Cancer Ther 2009;8(4):980–7]

Introduction

Lung cancer is the most common cause of cancer-related mortality. In current clinical practice, chemotherapy is used in combination with radiotherapy as an adjuvant or neoadjuvant therapy. Moreover, combination chemotherapy is regarded as the standard care in the treatment of unresectable locally advanced (stage IIIB), metastatic (stage IV), or recurrent disease. Although there have been major improvements over recent decades in surgical techniques and the role of chemotherapy-radiotherapy in the treatment of non–small cell lung cancer, the long-term outlook for such patients has not changed significantly. The median survival for patients with advanced-stage non–small cell lung cancer treated with platinum-based chemotherapy is a disappointing 8 to 10 months (1). Clearly, new therapies are needed that are capable of treating such advanced cancers in addition to preventing their formation.

One type of cancer therapy that has been extensively investigated is virotherapy, which uses oncolytic viruses engineered to selectively replicate within tumor cells, killing them. We previously developed an adenovirus vector that drives the *E1A* and *E1B* genes under the hTERT promoter, designated OBP-301 (Telomelysin), and showed its selective replication, as well as its profound cytotoxic activity, in a variety of human cancer cells (2–5). Although the development of OBP-301 as a monotherapy is currently under way clinically based on the promising preclinical results, multimodal strategies to enhance antitumor efficacy *in vivo* are essential for successful clinical outcome. In fact, most clinical trials for oncolytic viruses have been conducted in combination with chemotherapy or radiotherapy (6).

Gemcitabine (2,2-difluorodeoxycytidine) is a third-generation agent that has been developed in the past decades. Gemcitabine is a deoxycytidine analogue that has shown efficacy as a treatment for many solid tumors and is now extensively used in the treatment of patients with various tumor types (7, 8), but inherent and acquired resistance has resulted in low response rates. In the present study, we hypothesized that combination of oncolytic adenoviral agents (with novel mechanisms of action) with

Received 9/19/08; revised 12/15/08; accepted 1/20/09.

Grant support: Ministry of Education, Science, and Culture, Japan (T. Fujiwara); Ministry of Health and Welfare, Japan (T. Fujiwara); and Japan China Medical Association (D. Liu).

The costs of publication of this article were defrayed in part by the payment of page charges. This article must therefore be hereby marked *advertisement* in accordance with 18 U.S.C. Section 1734 solely to indicate this fact.

Requests for reprints: Toshiyoshi Fujiwara, Center for Gene and Cell Therapy, Okayama University Hospital, 2-5-1 Shikata-cho, Okayama 700-8558, Japan. Phone: 81-86-235-7997; Fax: 81-86-235-7884. E-mail: toshi_f@md.okayama-u.ac.jp

doi:10.1158/1535-7163.MCT-08-0901

chemotherapeutic agents could improve the antitumor effects and minimize the toxic side effects of the latter by reducing the concentrations of anticancer drugs. To test our hypothesis, we examined the therapeutic effects of OBP-301 combined with gemcitabine both *in vitro* and *in vivo*. The results showed that combination therapy with OBP-301 and gemcitabine produced therapeutic benefits over either individual modality.

Materials and Methods

Cell Lines and Cell Cultures

The human large cell lung cancer cell line H460, the bronchioloalveolar carcinoma cell line H322, and the bronchioloalveolar carcinoma cell line H358 were propagated in monolayer culture in RPMI 1640 supplemented with 10% FCS.

Chemotherapeutic Agents and Viruses

Gemcitabine (Gemzar) was obtained from Eli Lilly Co. Stock solution was prepared in 0.9% NaCl and the agent was further diluted in growth medium immediately before use. OBP-301 is a telomerase-specific replication-competent adenovirus variant, in which the hTERT promoter element drives the expression of *E1A* and *E1B* linked with internal ribosomal entry site. The virus was purified by ultracentrifugation in cesium chloride step gradients and titer was determined by plaque assay in 293 cells, as described previously (2–5).

Cell Viability Assay

2,3-Bis[2-methoxy-4-nitro-5-sulfophenyl]-2H-tetrazolium-5-carboxanilide inner salt (XTT) assay was done to assess the viability of tumor cells. H460, H322, and H358 cells at 1,000 per well were seeded onto 96-well plates at 18 to 20 h before viral infection. Cells were then infected with OBP-301 at low to high concentrations and were treated with fresh medium containing gemcitabine at various concentrations at 24 h after OBP-301 infection. Cell viability was determined at 4 d after treatment with OBP-301 and gemcitabine by using a Cell Proliferation Kit II (Roche Molecular Biochemicals) according to the protocol provided by the manufacturer.

In vitro Replication Assay

H460, H322, and H358 cells were seeded in six-well plates at 10^5 per well at 12 h before infection. Cells were infected with OBP-301 at a multiplicity of infection (MOI) of 10, 25, and 20 plaque-forming units (pfu)/cell, respectively, and fresh medium containing gemcitabine at 70 nmol/L for H460 cells, 100 nmol/L for H322 cells, and 3 nmol/L for H358 cells was then added at 24 h after infection. Cells were incubated at 37°C, trypsinized, and harvested for intracellular replication analysis at 2, 24, 48, 72, 96, and 108 h after OBP-301 infection. DNA purification was done using QIAmp DNA Mini kit (Qiagen, Inc.). The E1A DNA copy number was determined by quantitative real-time PCR using a LightCycler instrument and LightCycler-DNA Master SYBR Green I (Roche Diagnostics).

Assessment of E1A Expression by Western Blotting

H460, H322, and H358 cells infected with OBP-301 at an MOI of 10, 25, and 20, respectively, were collected at 5 d after infection, lysed in lysis buffer [10 mmol/L Tris-HCl (pH 7.5), 400 mmol/L NaCl, 1 mmol/L DTT, 5 mmol/L NaF, 1 mmol/L EDTA, 0.5% Na_3VO_4, 10% glycerol, 0.5% NP40, 0.1 mmol/L phenylmethylsulfonyl fluoride, 1 mg/mL leupeptin, 1 mg/mL aprotinin] for 30 min on ice, and centrifuged at 15,000 rpm for 30 min. Protein concentration was measured by means of the Bradford assay. Equal amounts of protein-containing sample buffer [62.5 mmol/L Tris-HCl (pH 6.8), 2% SDS, 10% glycerol, 5% β-mercaptoethanol] were boiled for 5 min and electrophoresed under reducing conditions on 12% (w/v) polyacrylamide gels. Proteins were electrophoretically transferred to Hybond polyvinylidene difluoride transfer membranes (Amersham) and incubated with primary antibody against E1A (BD Pharmingen) or rabbit anti-human β-actin monoclonal antibody (Sigma-Aldrich) followed by peroxidase-linked secondary antibody. An enhanced chemiluminescence Western system (Amersham) was used to detect secondary probes.

Cell Cycle Analysis

H460, H322, and H358 cells were infected with OBP-301 at 40, 100, and 80 MOI, respectively, for 24 h. The cells were then harvested and suspended in 1.5 mL PBS before fixing with ice-cold 70% ethanol for 30 min. Fixed samples were centrifuged for 5 min, and cell pellets were resuspended in 700 μL PBS containing RNase (0.25 mg/mL) followed by incubation for 30 min at 37°C. The volume was increased to 1 mL with PBS containing 1% bovine serum albumin and propidium iodide (50 μg/mL) and the suspensions were incubated at 4°C for 30 min. Stained cells were analyzed by FACScan (Becton Dickinson) and by WinMDI v2.8 software (Scripps Institute).

Assessment of Cell Cycle Regulator Protein Expression by Western Blotting

H460, H322, and H358 cells were infected with OBP-301 at 40, 100, and 80 MOI, respectively, before harvesting 24 h later. Collected cells were analyzed for expression of E2F1, p53, and E1A and phosphorylation of Akt. Primary antibodies were purchased from Santa Cruz Biotechnology (E2F1), Calbiochem Co. (p53), and Sigma Co. (β-actin). Protein expression was quantified by densitometric scanning using NIH Image software.

In vivo Human Tumor Model

H358 cells (5×10^6 per mouse) were injected s.c. into the backs of 5- to 6-wk-old female BALB/c *nu/nu* mice and were permitted to grow to 5 to 10 mm in diameter. At that time, mice were randomly assigned into four groups: mock, OBP-301, gemcitabine, and OBP-301 plus gemcitabine. Next, 50 μL of solution containing OBP-301 at a dose of 1×10^7 pfu/body or PBS were injected into the tumors. Simultaneously, each mouse in the combination group and gemcitabine group received an i.p. injection of 100 μL gemcitabine at a dose of 70 mg/kg every 3 d for three cycles starting at day 0. The perpendicular

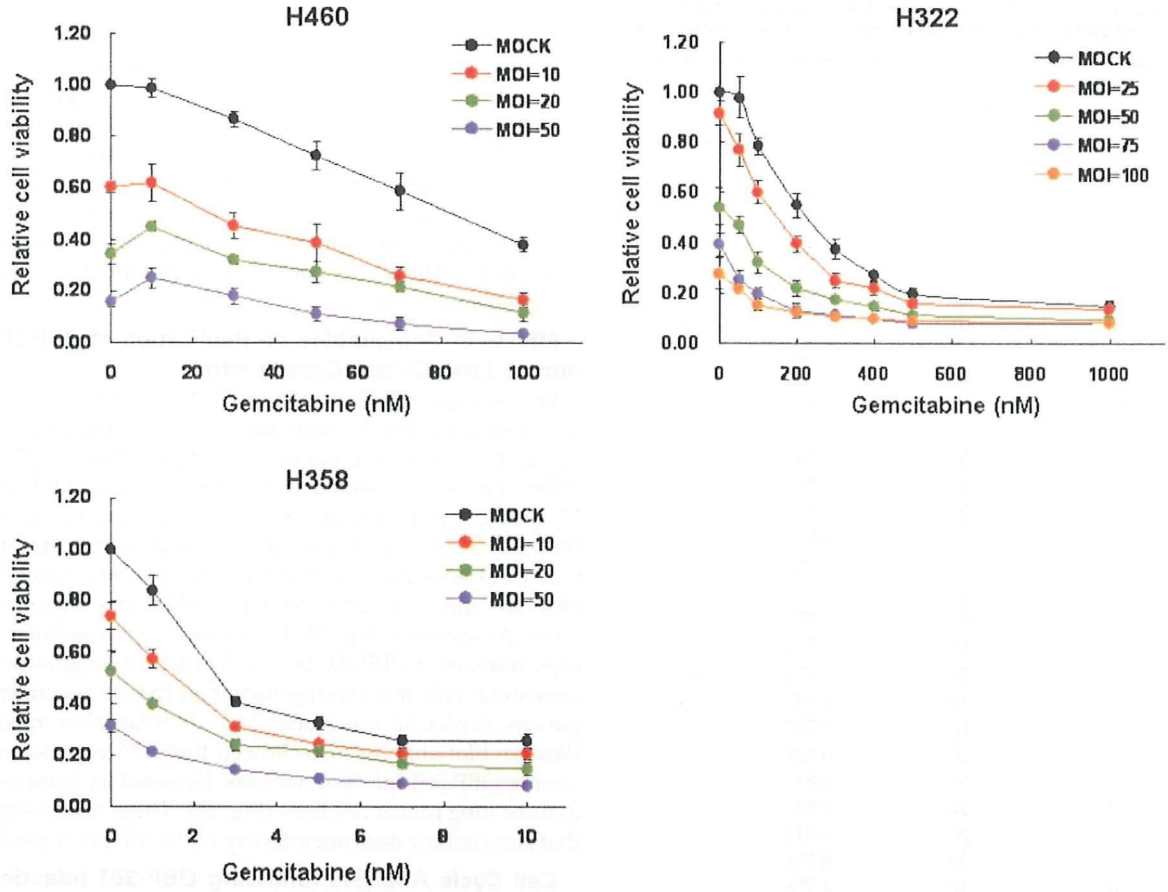

Figure 1. Combination efficiency of OBP-301 and gemcitabine on human lung cancer cell lines. H460, H322, and H358 cells were infected with OBP-301 at the indicated MOIs and then exposed to gemcitabine at the indicated concentrations at 24 h after infection. Cell viability was assessed by XTT assay at 5 d after OBP-301 infection. *Bars*, SD.

diameter of each tumor was measured every 3 d, and tumor volume was calculated using the following formula: tumor volume (mm^3) = $a \times b^2 \times 0.5$, where a is the longest diameter, b is the shortest diameter, and 0.5 is a constant used to calculate the volume of an ellipsoid. The experimental protocol was approved by the Ethics Review Committee for Animal Experimentation of Okayama University.

Statistical Analysis

Determinations of significant differences in mean tumor size among groups were assessed by calculating the value of Student's t using the original data analysis.

Results

Antitumor Efficacy of OBP-301 Combined with Gemcitabine in Human Lung Cancer Cell Lines *In vitro*

Before we tested the combination efficacy, sensitivity to gemcitabine and OBP-301 was evaluated in a variety of human lung cancer cell lines by the XTT method, and we selected three cell lines, H460, H322, and H358, for further experiments. From the XTT experiments with gemcitabine alone or OBP-301 alone (Supplementary Fig. S1),[5] the optimal concentrations of gemcitabine and OBP-301 were determined for each cell line. To examine the potential interaction between gemcitabine and OBP-301 *in vitro*, cell viability with six to eight different doses of OBP-301 and four to five doses of gemcitabine was then assessed by XTT assay at 5 days after treatment. Representative dose-response curves are shown in Fig. 1. All cell lines treated with OBP-301 and gemcitabine showed reduced viability when compared with cells treated with single agents.

We then used software to analyze the combination efficiency in these three cell lines (Table 1). In H358 cells, OBP-301 and gemcitabine were apparently synergistic at most doses, whereas the effect of the combination was mostly additive in H322 cells. In H460 cells, the effect was additive when the concentration of gemcitabine was 50 nmol/L; with the increasing of the concentration, however, a clear synergistic effect was seen. When the concentration was 100 nmol/L, synergism was apparent. These

[5] Supplementary data for this article are available at Molecular Cancer Therapeutics Online (http://mct.aacrjournals.org/).

Table 1. Combination index value analysis by CalcuSyn software (version 2) of combination efficiency in human lung cancer cells

Cells	Gemcitabine (nmol/L)	OBP-301 (MOI)	Combination index	Synergy
H460	10	10	1.261	−−
		20	1.405	−−
		50	1.688	−−
	30	10	0.996	±
		20	1.106	−
		50	1.349	−−
	50	10	1.037	±
		20	1.104	−
		50	0.998	±
	70	10	0.87	+
		20	1.037	±
		50	0.793	++
	100	10	0.793	++
		20	0.785	++
		50	0.531	+++
H358	1	10	0.952	±
		20	0.812	++
		50	0.772	++
	3	10	0.713	++
		20	0.674	+++
		50	0.641	+++
	5	10	0.792	++
		20	0.828	++
		50	0.613	+++
	7	10	0.88	+
		20	0.812	++
		50	0.596	+++
	10	10	1.178	−
		20	0.948	±
		50	0.693	+++
H322	50	25	1.028	±
		50	0.941	±
		75	0.874	++
		100	1.033	±
	100	25	0.953	±
		50	0.842	++
		75	0.848	++
		100	0.938	±
	200	25	0.944	±
		50	0.856	+
		75	0.82	++
		100	0.979	±
	300	25	0.912	±
		50	1.024	±
		75	0.887	+
		100	0.887	+
	400	25	1.005	±
		50	0.975	±
		75	1.093	±
		100	0.938	±
	500	25	0.977	±
		50	0.97	±
		75	0.946	±
		100	1.154	−

NOTE: Range of combination index symbol descriptions: 0.3 to 0.7, +++, synergism; 0.7 to 0.85, ++, moderate synergism; 0.85 to 0.90, +, slight synergism; 0.90 to 1.10, ±, additive; 1.10 to 1.20, −, slight antagonism; 1.20 to 1.45, −−, moderate antagonism.

results suggest that combination treatment with OBP-301 plus gemcitabine was effective in all cell lines tested.

We also assessed the morphologic changes in cells treated with either the combination modality or single agents. Phase-contrast images at 96 hours after OBP-301 infection showed the growth of cells to subconfluence without morphologic changes in the presence of gemcitabine, whereas a rapid loss of viability due to massive cell death, as evidenced by ballooning and floating cells, was evident when gemcitabine was combined with OBP-301 infection (Supplementary Fig. S2).[5]

Effects of Gemcitabine on Replication of OBP-301 in Human Lung Cancer Cells *In vitro*

We used quantitative real-time PCR and Western blotting to assess the effects of gemcitabine on replication of OBP-301 in the three lung cancer cell lines. H460, H322, and H358 cells were infected with OBP-301 at an MOI of 10, 25, and 20, respectively, and were then treated with 70, 100, and 3 nmol/L of gemcitabine at 24 hours after infection. Cells were harvested at the indicated time points after OBP-301 infection, and extracted DNA was subjected to assay. As shown in Fig. 2A, the increase in intracellular viral copy number of OBP-301 by 4 to 5 orders of magnitude was consistent with or without gemcitabine in both treatment regimens. A plateau was reached at ~48 hours after infection. Western blot analysis also showed that E1A expression following OBP-301 infection was not hindered by gemcitabine in three lung cancer cell lines (Fig. 2B). These results suggest that gemcitabine does not interfere with OBP-301 replication.

Cell Cycle Analysis following OBP-301 Infection in Human Lung Cancer Cells

To further explore the "greater than additive response" observed when cells were infected with OBP-301 followed by gemcitabine treatment, we carried out cell cycle analysis of these cells after OBP-301 infection by flow cytometric analysis of propidium iodide–stained cells, a measure of DNA content. As shown in Fig. 3A, the cell cycle distribution apparently changed compared with mock-infected cells at 24 hours after OBP-301 infection in all cell lines tested, although there was no increase in the sub-G_0-G_1 population indicating apoptotic cell death. The number of cells in S phase increased from 43.85% to 56.41% in H460 cells, from 46.72% to 67.09% in H322 cells, and from 38.22% to 57.67% in H358 cells (Table 2). These results suggest that OBP-301 is able to accumulate infected cells in S phase, which may render cells more sensitive to gemcitabine.

Changes in Cell Cycle Regulator Protein Expression following OBP-301 Infection

To clarify the mechanisms of cell cycle regulation by OBP-301, we analyzed the expression of proteins that have a crucial role in the cell cycle. H460, H322, and H358 cells were infected with OBP-301 at an MOI of 40, 100, and 80, and Western blot analysis was then done 24 hours later. As shown in Fig. 3B, expression levels of E2F1, as well as phosphorylated Akt, greatly increased after OBP-301 infection compared with the mock-infected controls in all three cell lines. p53 protein expression was not detectable in H460

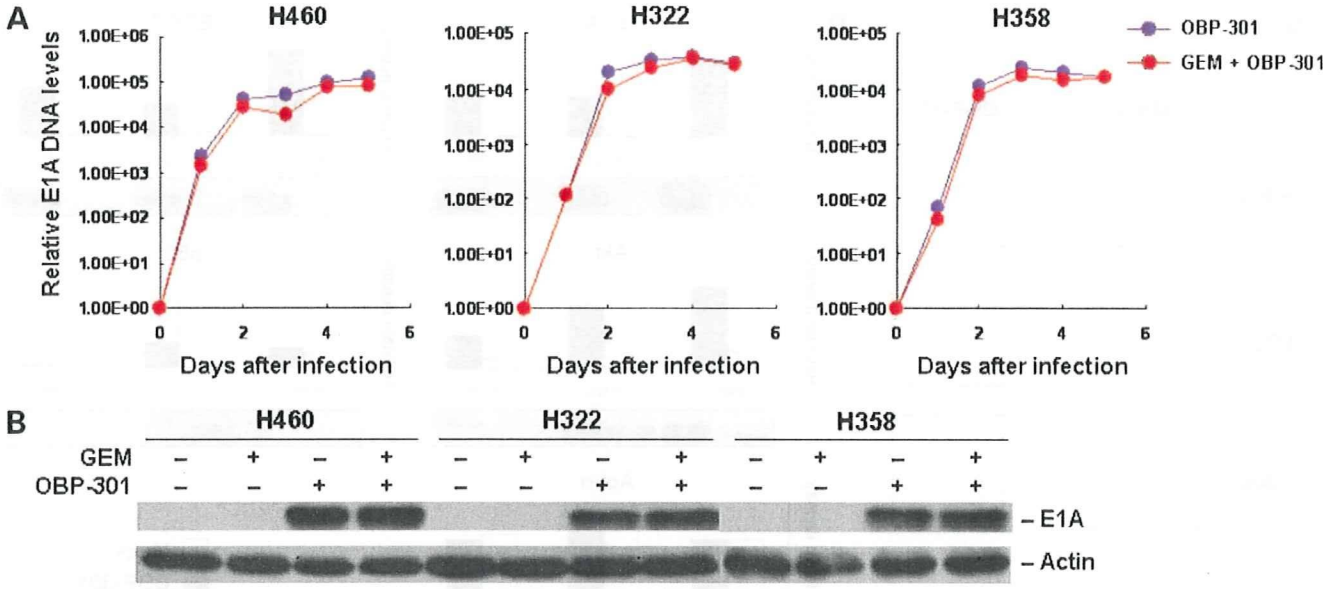

Figure 2. Assessment of viral DNA replication in human lung cancer cells. **A,** H460, H322, and H358 cells were infected with OBP-301 at an MOI of 10, 25, and 20, respectively, for 2 h as a baseline for virus DNA levels. Following the removal of virus inocula at 24 h after the infection, H460, H322, and H358 cells were further incubated with 70, 100, and 3 nmol/L of gemcitabine (*GEM*), respectively, for the indicated periods of time. Cells were then subjected to quantitative real-time PCR assay. Viral E1A copy number was defined as the fold increase for each sample relative to that at 2 h (2 h = 1). **B,** Western blot analysis of E1A expression in human lung cancer cells. Cells were treated with OBP-301, gemcitabine, or a combination of both, as described above, and then subjected to assay at 4 d after infection.

expressing the wild-type *p53* gene and p53-null H358 cells, whereas OBP-301 infection down-regulated mutant p53 expression in H322 cells.

Antitumor Effects of OBP-301 plus Gemcitabine in Human Lung Cancer Xenografts

Finally, we assessed the therapeutic efficacy of OBP-301 in combination with gemcitabine against H358 human lung cancer cells *in vivo*. H358 cells were implanted as xenografts into the hind flanks of *nu/nu* mice. Mice bearing palpable H358 tumors measuring 5 to 7 mm in diameter received simultaneous treatment of intratumoral injection of either 10^7 pfu OBP-301 or PBS plus i.p. administration of either 70 mg/kg gemcitabine or PBS every 3 days for three cycles starting at day 0. As shown in Fig. 4, administration of gemcitabine resulted in significant tumor growth suppression compared with mock-treated tumors for 34 days after initiation of treatment ($P < 0.05$); the combination of OBP-301 plus gemcitabine, however, produced a more profound and significant inhibition of tumor growth compared with mice treated with gemcitabine alone for at least 45 days ($P < 0.05$). The addition of OBP-301 clearly prolonged the antitumor effects of gemcitabine. Intratumoral injection of a replication-deficient adenovirus with or without systemic administration of gemcitabine had no apparent effect on the growth of H358 tumors (data not shown).

Discussion

Replication-competent oncolytic adenoviruses are promising as a novel anticancer therapy (9). In our laboratory, a tumor-specific replication-selective adenovirus, designated Telomelysin or OBP-301, is effective against human cancers (2–5). This virus was genetically designed to replicate under the control of hTERT promoter specifically in tumor cells, causing specific oncolysis. Despite the encouraging outcomes in animal experiments, combination chemotherapy and virotherapy are recommended in clinical treatment, as tumor progression is very rapid in most patients. In the current study, we explored the combination effects of OBP-301 and gemcitabine in human lung cancer cells *in vitro* and *in vivo*.

Adenovirus therapy combined with gemcitabine has been reported in the treatment of pancreatic cancer. Halloran et al. (9) reported that incubation of Panc-1 cells with either 5-fluorouracil or gemcitabine followed by adenovirus-mediated overexpression of $p16^{INK4A}$ resulted in a substantial reduction in cell viability under conditions where the drugs alone had minimal cytotoxicity. Although most studies reporting the combination effects of gemcitabine and adenoviral agents for pancreatic tumor used therapeutic genes critical for tumor growth inhibition, OBP-301 itself is an effective oncolytic virus and leads to infected cell destruction. Moreover, it has been reported that the type 5 adenoviral E1A sensitizes hepatocellular carcinoma cells to gemcitabine (10). These observations support the notion that oncolytic adenoviruses combined with gemcitabine are a rational modality for the treatment of human cancer.

The antitumor efficacy of OBP-301 was found to be enhanced when combined with gemcitabine in human lung cancer cells *in vitro* (Fig. 1; Table 1). Synergistic interaction was apparent in H460 and H358 cells; the combination

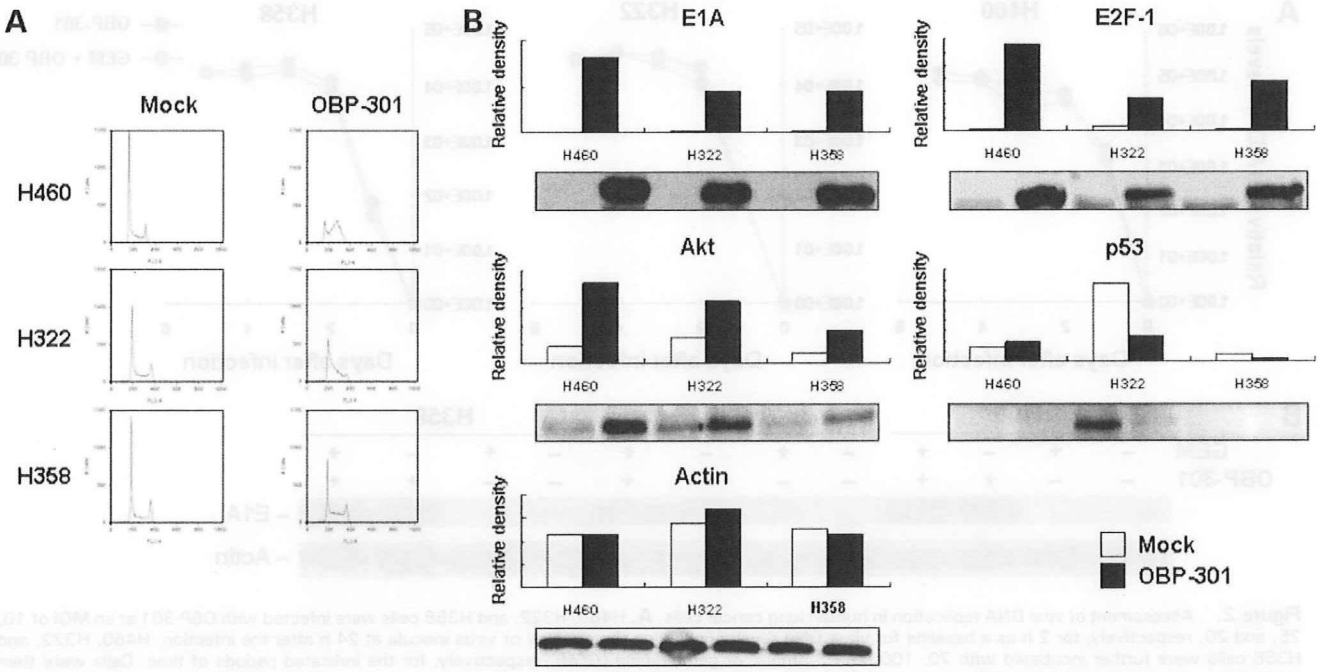

Figure 3. Cell cycle analysis and Western blotting of cell cycle regulator protein following OBP-301 infection in human lung cancer cells. **A,** H460, H322, and H358 cells were infected with OBP-301 at an MOI of 40, 100, and 80 MOI, respectively. DNA content was determined by propidium iodide staining and flow cytometric analysis at 24 h after OBP-301 infection. **B,** H460, H322, and H358 cells were either mock infected or infected with OBP-301 at an MOI of 40, 100, and 80 MOI, respectively. Following the removal of virus inocula, cells were collected at 24 h after infection and subjected to analysis. Equivalent amounts of protein obtained from whole-cell lysates were loaded into each lane, probed with primary antibodies, and then visualized using an enhanced chemiluminescence detection system. Equal loading of samples was confirmed by reprobing with antiactin antiserum. Protein expression was quantified by densitometric scanning using NIH Image software.

effect, however, was additive in H322 cells, suggesting that the effect of the combination is dependent on cell type. We also confirmed that this synergistic effect could be observed in human pancreatic cancer cells (Supplementary Fig. S3).[5] Gemcitabine is a deoxycytidine analogue and the incorporation of gemcitabine triphosphate into DNA causes chain termination, which is the major mechanism underlying the cytotoxicity of gemcitabine (11). Although there was concern over whether gemcitabine would interrupt the viral replication of OBP-301, quantitative real-time PCR analysis showed that intracellular replication of OBP-301 was not affected by gemcitabine (Fig. 2). The cytotoxic mechanisms of OBP-301 are distinct from those of gemcitabine, and therefore, combination effects could be observed provided that gemcitabine does not inhibit viral replication.

To clarify the mechanisms of the greater than additive response, cell cycle analysis was done following OBP-301 infection. Cells treated with OBP-301 tended to accumulate in the S phase at 24 hours after infection (Fig. 3A; Table 2). It has been reported that many DNA viruses can drive quiescent cells through G_1 into S phase by the expression of viral proteins (12–14). During the early phase of the adenovirus infection, the host cell is transformed into an efficient producer of the viral genome. The first gene that is transcribed in the viral genome is *E1A*, which can bind to numerous cellular proteins and acts as a multifunctional protein. Our data showed that OBP-301 infection increases the phosphorylation of Akt, as well as E2F1 expression, in all three human lung cancer cell lines (Fig. 3B). These effects are thought to be due to adenoviral E1A protein expression, as the dl312 adenovirus lacking the E1 genes did not phosphorylate Akt (data not shown).

Direct evidence of cell cycle promotion by Akt was seen when coexpression of Akt rescued cells from PTEN-induced cell cycle arrest (15). Retinoblastoma (Rb) protein restrains proliferation, in part, by modulating the activity of E2F

Table 2. Cell cycle analysis after OBP-301 infection in human lung cancer cells

Cell lines	Treatment	Cell cycle		
		G_1 (%)	S (%)	G_2 (%)
H460	Mock	43.54	43.85	8.61
	OBP-301	10.91	56.41	32.54
H322	Mock	40	46.72	10.85
	OBP-301	27.49	67.09	3.23
H358	Mock	45.89	38.22	14.29
	OBP-301	28.93	57.67	11.45

NOTE: H460, H322, and H358 cell lines were treated with OBP-301 at 40, 100, and 80 MOI, respectively. Cells were then subjected to cell cycle analysis at 24 h after treatment by the fluorescence-activated cell sorting method. The percentages of cells in the G_1, S, and G_2 phases are shown.

A

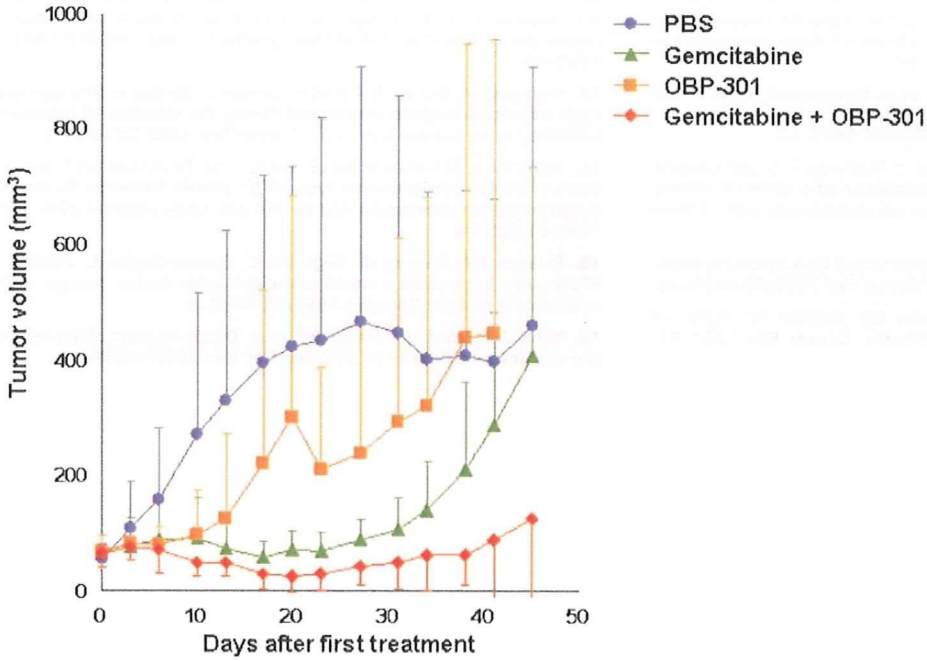

Figure 4. Antitumor effects of intratumorally injected OBP-301 and i.p. administered gemcitabine against established back H358 xenograft tumors in *nu/nu* mice. **A,** H358 tumor cells (5×10^6/each) were s.c. injected into the right flanks of mice. OBP-301 (1×10^8 pfu/body) and gemcitabine (70 mg/kg) were administered intratumorally and i.p., respectively, for three cycles every 3 d. PBS was used as the control. Eight mice were used for each group. Tumor growth is expressed as mean volume ± SE. **B,** statistical analysis was done using Student's *t* test for differences among indicated groups. Statistical significance (*red number*) was defined as $P < 0.05$.

B

	Day 23	Day 27	Day 31	Day 34	Day 38	Day 41	Day 45
PBS vs OBP-301	0.116	0.172	0.354	0.588	0.870	0.788	0.774
PBS vs Gemcitabine (GEM)	0.015	0.025	0.028	0.021	0.073	0.336	0.773
PBS vs GEM + OBP-301	0.009	0.014	0.014	0.005	0.004	0.008	0.051
OBP-301 vs GEM	0.034	0.068	0.101	0.155	0.198	0.377	0.594
OBP-301 vs OBP-301 + GEM	0.011	0.024	0.021	0.050	0.044	0.054	0.080
GEM vs OBP-301 + GEM	0.013	0.007	0.022	0.029	0.015	0.012	0.033

transcription factors. In quiescent cells, Rb associates with several E2Fs, resulting in the repression of proliferation-associated genes. As cells progress into the cell cycle, cyclin-dependent kinases phosphorylate Rb, freeing E2F and allowing it to directly transactivate genes required for S-phase entry (16). In fact, replication-deficient adenovirus-mediated *E2F1* gene transfer into human cancer cells resulted in accumulation of an S-phase cell population (Supplementary Fig. S4).[5] Thus, OBP-301 infection expressed E1A protein, which in turn up-regulated the expression of phosphorylated Akt and E2F1, leading to cell cycle promotion and S-phase entry presumably by the deactivation of Rb. Indeed, we confirmed that OBP-301 infection decreased Rb protein expression in H460 cells (data not shown). The accumulation of the tumor cells in S phase increases the cytotoxicity of gemcitabine, which kills cells in S phase.

In summary, our data show that telomerase-specific oncolytic adenovirus infection increases the sensitivity of human lung cancer cells to gemcitabine due to S-phase accumulation. The combination of OBP-301 and gemcitabine efficiently inhibits human cancer cell growth both *in vitro* and *in vivo*, an outcome that has important implications for tumor-specific oncolytic chemovirotherapies for human lung cancer.

Disclosure of Potential Conflicts of Interest

M. Ouchi, H. Onimatsu, and Y. Urata: employees of Oncolys BioPharma, Inc. T. Fujiwara: consultant for Oncolys BioPharma, Inc. No other potential conflicts of interest were disclosed.

Acknowledgments

We thank Daiju Ichimaru and Hitoshi Kawamura for their helpful discussions and Tomoko Sueishi for her excellent technical support.

References

1. Gkiozos I, Charpidou A, Syrigos K. Developments in the treatment of non-small cell lung cancer. Anticancer Res 2007;27:2823–7.

2. Kawashima T, Kagawa S, Kobayashi N, et al. Telomerase-specific replication-selective virotherapy for human cancer. Clin Cancer Res 2004;10:285–92.

3. Taki M, Kagawa S, Nishizaki M, et al. Enhanced oncolysis by a tropism-modified telomerase-specific replication-selective adenoviral agent OBP-405 ('Telomelysin-RGD'). Oncogene 2005;24:3130–40.

4. Hashimoto Y, Watanabe Y, Shirakiya Y, et al. Establishment of biological and pharmacokinetic assays of telomerase-specific replication-selective adenovirus. Cancer Sci 2008;99:385–90.

5. Endo Y, Sakai R, Ouchi M, et al. Virus-mediated oncolysis induces danger signal and stimulates cytotoxic T-lymphocyte activity via proteasome activator upregulation. Oncogene 2008;27:2375–81.

6. Khuri FR, Nemunaitis J, Ganly I, et al. A controlled trial of intratumoral ONYX-015, a selectively-replicating adenovirus, in combination with cisplatin and 5-fluorouracil in patients with recurrent head and neck cancer. Nat Med 2000;6:879–85.

7. Paz-Ares L, Douillard JY, Koralewski P, et al. Phase III study of gemcitabine and cisplatin with or without aprinocarsen, a protein kinase C-α antisense oligonucleotide, in patients with advanced-stage non-small-cell lung cancer. J Clin Oncol 2006;24:1428–34.

8. Heinemann V, Quietzsch D, Gieseler F, et al. Randomized phase III trial of gemcitabine plus cisplatin compared with gemcitabine alone in advanced pancreatic cancer. J Clin Oncol 2006;24:3946–52.

9. Halloran CM, Ghaneh P, Shore S, et al. 5-Fluorouracil or gemcitabine combined with adenoviral-mediated reintroduction of p16INK4A greatly enhanced cytotoxicity in Panc-1 pancreatic adenocarcinoma cells. J Gene Med 2004;6:514–25.

10. Lee WP, Tai DI, Tsai SL, et al. Adenovirus type 5 E1A sensitizes hepatocellular carcinoma cells to gemcitabine. Cancer Res 2003;63:6229–36.

11. Huang P, Chubb S, Hertel LW, Grindey GB, Plunkett W. Action of 2',2-difluorodeoxycytidine on DNA synthesis. Cancer Res 1991;51:6110–7.

12. Wang HG, Draetta G, Moran E. E1A induces phosphorylation of the retinoblastoma protein independently of direct physical association between the E1A and retinoblastoma products. Mol Cell Biol 1991;11:4253–65.

13. Hollyoake M, Stühler A, Farrell P, Gordon J, Sinclair A. The normal cell cycle activation program is exploited during the infection of quiescent B lymphocytes by Epstein-Barr virus. Cancer Res 1995;55:4784–7.

14. Morozov A, Shiyanov P, Barr E, Leiden JM, Raychaudhuri P. Accumulation of human papillomavirus type 16 E7 protein bypasses G_1 arrest induced by serum deprivation and by the cell cycle inhibitor p21. J Virol 1997;71:3451–7.

15. Paramio JM, Navarro M, Segrelles C, Gomez-Casero E, Jorcano JL. PTEN tumor suppressor is linked to the cell-cycle control through the retinoblastoma protein. Oncogen 1999;18:7462–8.

16. Nahle Z, Polakoff J, Davuluri RV, et al. Direct coupling of the cell cycle and cell death machinery by E2F. Nat Cell Biol 2002;4:859–64.

In vivo internal tumor illumination by telomerase-dependent adenoviral GFP for precise surgical navigation

Hiroyuki Kishimoto[a,b,c], Ming Zhao[a], Katsuhiro Hayashi[a,b], Yasuo Urata[d], Noriaki Tanaka[c], Toshiyoshi Fujiwara[c,e], Sheldon Penman[f,1], and Robert M. Hoffman[a,b,1]

[a]AntiCancer, Inc., San Diego, CA 92111; [b]Department of Surgery, University of California, San Diego, CA 92103-8220; [c]Division of Surgical Oncology, Department of Surgery, Okayama University Graduate School of Medicine, Dentistry and Pharmaceutical Sciences, Okayama 700-8558, Japan; [d]Oncolys BioPharma, Inc., Tokyo 106-0032, Japan; [e]Center for Gene and Cell Therapy, Okayama University Hospital, Okayama 700-8558, Japan; and [f]Department of Biology, Massachusetts Institute of Technology, Cambridge, MA 02139-4307

Contributed by Sheldon Penman, June 8, 2009 (sent for review May 10, 2009)

Cancer surgery requires the complete and precise identification of malignant tissue margins including the smallest disseminated lesions. Internal green fluorescent protein (GFP) fluorescence can intensely illuminate even single cells but requires *GFP* sequence transcription within the cell. Introducing and selectively activating the *GFP* gene in malignant tissue in vivo is made possible by the development of OBP-401, a telomerase-dependent, replication-competent adenovirus expressing GFP. This potentially powerful adjunct to surgical navigation was demonstrated in 2 nude mouse models that represent difficult surgical challenges—the resection of widely disseminated cancer. HCT-116, a model of intraperitoneal disseminated human colon cancer, was labeled by virus injection into the peritoneal cavity. A549, a model of pleural dissemination of human lung cancer, was labeled by virus administered into the pleural cavity. Only the malignant tissue fluoresced brightly in both models. In the intraperitoneal model of disseminated cancer, fluorescence-guided surgery enabled resection of all tumor nodules labeled with GFP by OBP-401. The data in this report suggest that adenoviral-GFP labeling tumors in patients can enable fluorescence-guided surgical navigation.

Adenovirus | green fluorescent protein | metastasis

The intent of cancer surgery is to remove malignant tissue together with margins of presumably normal tissue (1–3) to ensure complete removal of abnormal cells. Estimating margin width during surgery is critical and depends on the surgeon's vision. There have been many developments intended to improve the delineation of tissue margins using morphologic and optical differences between normal and abnormal tissue. This report describes a major enhancement of cancer surgical navigation using the selective fluorescent labeling, in vivo, of malignant tissue. Bright GFP fluorescence clearly illuminates the tumor boundaries and facilitates detection of the smallest disseminated disease lesions.

Highly selective viral replication in malignant cells growing in normal tissue has recently become possible using novel adenoviruses, OBP-301 (4–6) and, more recently, OBP-401 (7, 8). This latter virus, which can enter most cells, contains the replication cassette with the human telomerase reverse transcriptase (hTERT) promoter driving the expression of the viral *E1* genes, and the inserted *GFP* gene. Virus replication and, hence, *GFP* gene expression occur only in the presence of an active telomerase, i.e., in malignant tissue (7). The OBP-401 virus was first tested by injection directly into HT-29 human colon tumors orthotopically implanted into the rectum in BALB/c *nu/nu* mice (7). Subsequent para-aortic lymph node metastasis was observed by laparotomy under fluorescence. The adaption of GFP fluorescence to in vivo labeling of tumor tissue should facilitate precision surgical navigation in live animals and, very possibly, in a clinical surgical setting.

Results

Fluorescence Labeling of Human Cancer Cells with OBP-401 in Vitro. A549 tumor cells, growing in tissue culture, were infected with OPP-401, and the development of GFP fluorescence followed. The fluorescence intensity gradually increased after infection as the virus, with its *GFP* gene, replicated (Fig. 1*A*).

The extent of infection was tested by infecting red fluorescent protein (RFP)-expressing cancer cells, growing in cell culture, with OBP-401. These included A549-RFP, PC-3-RFP, HCT-116-RFP, and HT-29-RFP cells. In most cells, the introduction of green fluorescence changes the cell color from red to yellow, showing that most were infected by OBP-401. Any remaining red fluorescence clearly identifies those few cells that remain uninfected by the adenovirus. The color changes increased gradually followed by cell death due to the cytopathic effect of replicating OBP-401 (Fig. 1 *B* and *C*).

Fluorescence Labeling of Subcutaneous Tumors by Infection in Vivo with OBP-401. Both nonfluorescent PC-3 and red fluorescent PC-3-RFP human prostate cancer cells were inoculated s.c. (Fig. 2 *A* and *B*). The resulting s.c. tumors were injected with 1×10^8 plaque-forming units (PFU) of OBP-401 as shown in Fig. 2*B*. A color change from red to yellow in the s.c. PC-3-RFP tumor and the onset of GFP fluorescence in the nonfluorescent PC-3 tumor were observed by the third day after virus injection (Fig. 2*C*). An RFP filter selectively showed the tumors' endogenous RFP fluorescence (Fig. 2*D*). Similarly, a GFP filter showed GFP fluorescence induced in the tumors by OBP-401 (Fig. 2*E*). Infecting tumor cells that are endogenously expressing RFP with the GFP-expressing adenoviral vector OBP-401 clearly shows the extent of GFP labeling of the tumor. Cells showing a yellow fluorescence are infected with OBP-401, while the remaining red fluorescent cells clearly indicate the small portion that might remain uninfected.

Labeling Peritoneal Carcinomatosis with OBP-401. Peritoneal carcinomatosis was induced in the abdominal cavity of nude mice by inoculating 3×10^6 red fluorescent HCT-116-RFP human colorectal cancer cells. Various sized peritoneal disseminated nodules developed within 12 days. These were clearly visible by fluorescence imaging using a long-pass filter and/or a specific RFP filter (Fig. 3 *A* and *B*). Even very small disseminated nodules were illuminated by RFP fluorescence (Fig. 3*B*). Although there was some autofluorescence from adjacent organs visible, the tumor nodules were not visible through a GFP filter (Fig. 3 *A* and *B*).

Author contributions: H.K., Y.U., N.T., T.F., and R.M.H. designed research; H.K., M.Z., and K.H. performed research; H.K., Y.U., N.T., T.F., S.P., and R.M.H. analyzed data; and H.K., S.P., and R.M.H. wrote the paper.

The authors declare no conflict of interest.

[1]To whom correspondence may be addressed. E-mail: penman@mit.edu or all@anticancer.com.

www.pnas.org/cgi/doi/10.1073/pnas.0906388106

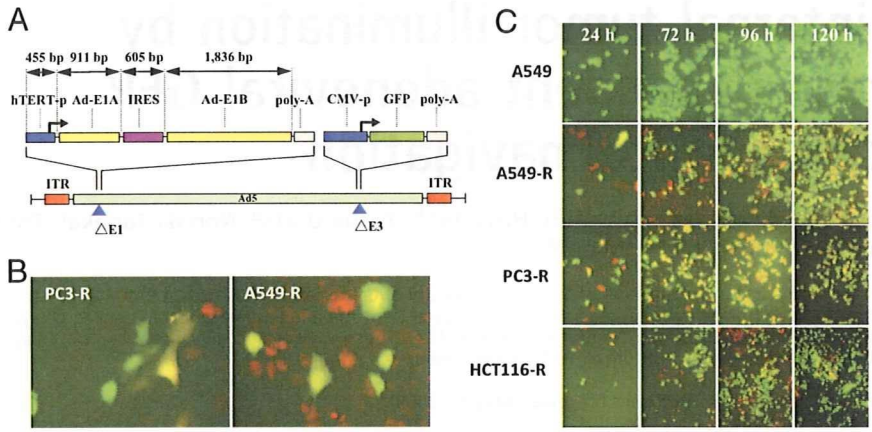

Fig. 1. Structure of OBP-401, virus replication in human cancer cells and induced GFP expression. (*A*) Schematic DNA structure of OBP-401. OBP-401 is a telomerase-specific replication-competent adenovirus variant, in which the hTERT promoter element drives the expression of *E1A* and *E1B* genes linked with an IRES. The *GFP* gene is inserted under the CMV promoter into the E3 region. (*B*) A549-RFP and PC-3-RFP cells changed color after infection with OBP-401 at a multiplicity of injection (MOI) of 10. (Magnification, 200×.) (*C*) Noncolored A549 as well as RFP-expressing cancer cells A549-RFP, PC-3-RFP, and HCT-116-RFP were infected with OBP-401 at an MOI of 10. Cells were assessed at indicated time points for GFP expression under fluorescence microscopy. After OBP-401 infection, noncolored A549 cells expressed GFP fluorescence. In A549-RFP, PC-3-RFP, and HCT-116-RFP, color changes from red to yellow were detected. The color changes increased gradually in a time-dependent fashion. (Magnification, 200×.)

Once the malignant nodules were established at 12 days after intraperitoneal (i.p.) implantation of HCT-116-RFP cells, 1×10^8 PFU OBP-401 were injected into the mouse abdominal cavity. Selective color filters showed that the HCT-116-RFP disseminated nodules expressed GFP fluorescence as well as RFP when examined 5 days later (Fig. 3*C*). RFP fluorescence

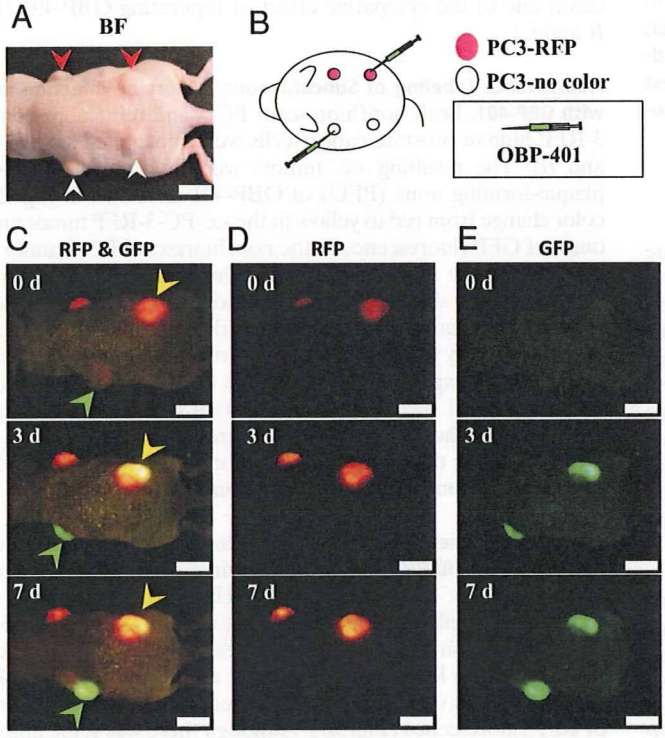

Fig. 2. Selective visualization of s.c. tumors in vivo after OBP-401 GFP-labeling. s.c. tumors of noncolored PC-3 (*A*, white arrowheads) or PC-3-RFP (*A*, red arrowheads) human prostate cancer cells were intratumorally injected with PBS for control or OBP-401 at a dose of 1×10^8 PFU as shown in *B*. After intratumoral injection of OBP-401, GFP fluorescence was detected in noncolored PC-3 s.c. tumors (*C*, green arrowheads) and a color change from red to yellow was also observed in PC-3-RFP tumors by fluorescence imaging using a long-pass filter to simultaneously observe both GFP and RFP (*C*, yellow arrowheads). With specific filters, the tumors endogenous RFP fluorescence (*D*) and GFP fluorescence induced by OBP-401 (*E*) were individually detected. (Scale bar, 10 mm.)

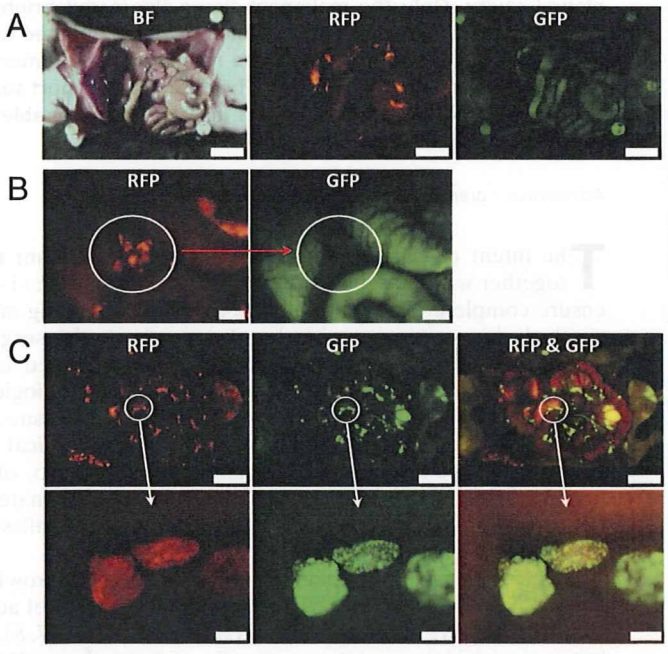

Fig. 3. Intraperitoneal injection of OBP-401 visualized peritoneal dissemination of HCT-116-RFP cells. (*A*) HCT-116-RFP human colorectal cancer cells were inoculated into the abdominal cavity of nude mice. Various sized disseminated peritoneal nodules appeared within 12 days. (Scale bar, 10 mm.) (*B*) At higher magnification, peritoneally disseminated nodules of HCT-116-RFP were clearly visible using a specific filter for RFP (*Left*), and these nodules did not express GFP (*Right*). (Scale bar, 2 mm.) (*C*) Mice with HCT-116-RFP peritoneal disseminated nodules were i.p. injected with OBP-401 at a dose of 1×10^8 PFU. Five days after virus administration, HCT-116-RFP peritoneal-disseminated nodules were detected with their endogenous RFP fluorescence (*Left*). These disseminated nodules now expressed GFP fluorescence (*Middle*). With the long-pass filter, for simultaneous observation of both GFP and RFP, it can be seen that all of the RFP tumors were apparently labeled with GFP after OBP-401 injection (*Right*). (Scale bars: *Upper*, 10 mm; *Lower*, 500 μm.)

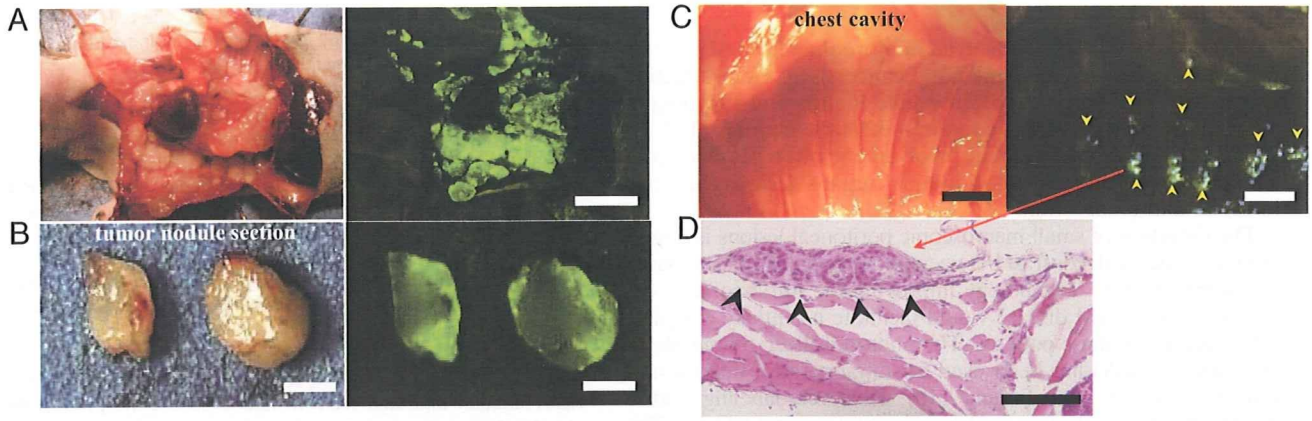

Fig. 4. Intrapleural injection of OBP-401 visualized pleural disseminations of A549 cells. (*A*) Two weeks after implantation of noncolored A549 cells into the thoracic space, OBP-401 at a dose of 1×10^8 PFU, was intrapleurally injected. Five days later, disseminated nodules were visualized by GFP fluorescence (*Right*). (Scale bar, 10 mm.) (*B*) Cross-section of pleural disseminated nodule. GFP expression was seen on the surface of pleurally disseminated nodules (*Right*). (Scale bar, 2 mm.) (*C*) Very small lesions that were not detectable in brightfield were visualized by GFP fluorescence (*Right*, arrowheads). (Scale bar, 2 mm.) (*D*) Histological analysis with H&E confirmed that these GFP-expressing lesions were adenocarcinomas (arrowheads). (Scale bar, 100 μm.)

was essentially coincident with that of GFP (Fig. 3*C*). These results indicate that i.p. injection of OBP-401 efficiently infected and labeled disseminated cancer.

Labeling of Pleurally Disseminated Cancer with OBP-401. These experiments assessed the effectiveness of OBP-401 labeling of pleural carcinomatosis in a mouse model of unlabeled A549 human lung cancer cells. The thoracic space of nude mice was inoculated with 2×10^6 cancer cells. Various sized disseminated plural nodules appeared within 10 days after implantation. At this time, 1×10^8 PFU of OBP-401 were injected into the thoracic cavity. Five days after injection of OBP-401, the cavity was examined using GFP fluorescence imaging. A representative mouse is shown in Fig. 4. Disseminated pleural nodules were visualized by GFP expression (Fig. 4 *A* and *B*). Even very small lesions, which are normally undetectable, were clearly illuminated by GFP fluorescence (Fig. 4*C*). Histological examination confirmed that these GFP-expressing tissues were adenocarcinomas. A representative histological section is shown in Fig. 4*D*. These results suggest that intrapleural injection of at least 1×10^8 PFU of OBP-401 can efficiently label disseminated pleural cancer. Lower doses of OBP-401 resulted in less efficient labeling.

OBP-401 Fluorescence-Guided Resection of Disseminated Peritoneal Tumors. In order to test the effectiveness of OBP-401-guided cytoreduction surgery, we used the peritoneal carcinomatosis model with nonfluorescent HCT-116 human colon cancer cells. Mice with peritoneal carcinomatosis were injected i.p. with OBP-401 at a dose of 1×10^8 PFU. Five days after viral administration, laparotomy was performed to remove intra-abdominal disease using fluorescence-guided navigation under anesthesia (Fig. 5 *A* and *B*). A representative mouse after cytoreduction surgery with OBP-401-navigation is shown in Fig. 5*C*. Disseminated cancer nodules, which would otherwise be undetectable, were clearly visible by bright GFP fluorescence. The resected nodules were visualized as frozen sections under both fluorescence (Fig. 5*D*) and after hematoxylin and eosin (H&E) staining (Fig. 5 *E* and *F*). These results suggest that OBP-401-labeling has significant potential for guiding cytoreduction surgery of disseminated cancer.

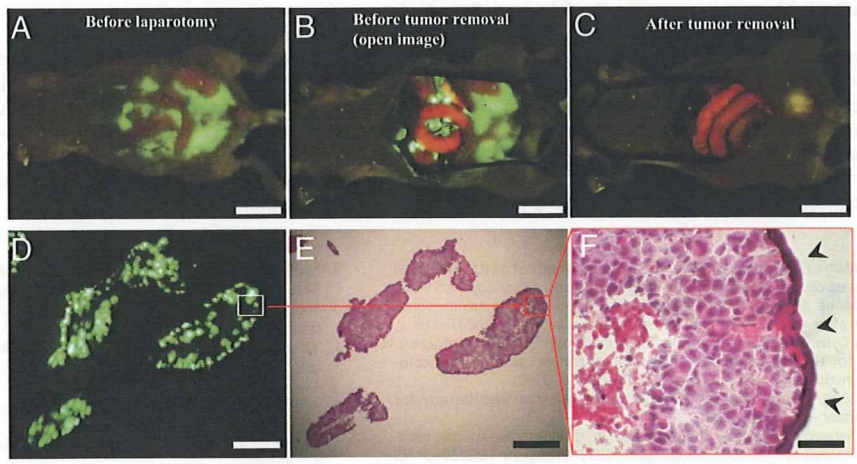

Fig. 5. Fluorescence-guided surgical removal of peritoneal disseminated HCT-116 tumors after GFP labeling with OBP-401. Noncolored HCT-116 human colon cancer cells were injected into the abdominal space of nude mice. Ten days later, 1×10^8 PFU of OBP-401 were i.p. injected. (*A*) Disseminated nodules were efficiently labeled and noninvasively visualized by GFP expression 5 days after virus administration. (*B*) Under general anesthesia, laparotomy was performed to remove intra-abdominal disease under GFP-guided navigation. (*C*) Disseminated nodules visualized by GFP-guided navigation were removed. (Scale bars: *A–C*, 10 mm.) (*D*) Frozen section of resected HCT-116 disseminated nodules with fluorescence detection. (Scale bar, 500 μm.) (*E*) H&E section of HCT-116 disseminated nodules shown in *D*. The box outlines a region of *D* and *E* analyzed in *F*. (Scale bar, 500 μm.) (*F*) Detail of the boxed region of *D* and *E*. (Scale bar, 50 μm.)

Discussion

The peritoneal surface is involved in more than 20% of patients with gastric, colon, and pancreatic cancers (1). Cytoreduction surgery requires resection of all visible tumors and stripping of all peritoneal surfaces that contain metastatic nodules (1, 2, 9). Therefore, visceral peritoneal involvement often requires concomitant resection of intra-abdominal organs such as the small intestine and colorectum.

The detection of small macroscopic peritoneal lesions is largely limited by the weak contrast between tumor nodules and surrounding normal tissues. Technology improving the intraoperative detection of peritoneal disease would facilitate essentially complete cytoreduction in these patients. The photosensitizer, 5-aminolevulinic acid (5-ALA) has been used for intraoperative detection of cancer lesions in neurosurgery (10). However, labeling that is essentially cancer-selective can be a powerful surgical adjunct. This report shows that OBP-401 infection of cancer cells leads to the highly selective induction of bright GFP fluorescence.

Implanting RFP-expressing cancer cell lines gave rise to fluorescent nodules whose color change clearly indicated the efficiency with which OBP-401 labeled disseminated peritoneal tumors with GFP. The change from red to yellow fluorescence indicated successful infection by OBP-401 (Fig. 3). Similarly, OBP-401 GFP labeling could detect dissemination nodules with high sensitivity in a pleural carcinomatosis model (Fig. 4).

Perhaps most importantly, we could remove disseminated disease in a peritoneal carcinomatosis model by using fluorescence-guided resection. These results suggest developing a dedicated excitation light for fluorescence-guided surgery similar to that described for use in mice (11). In the present study, during surgery, even very small peritoneal lesions could be identified with GFP fluorescence (11).

Materials and Methods

Recombinant Adenovirus. OBP-401, containing the *GFP* gene under the control of the CMV promoter with the hTERT promoter driving the *E1A* and *E1B* genes, was constructed as previously described (6, 7). OBP-401 was purified by ultracentrifugation in cesium chloride step gradients. Virus titers were determined by a plaque-forming assay using 293 cells. The virus was stored at −80°C.

Cell Culture. The human non-small cell lung cancer cell line A549, the human colorectal cancer cell lines HCT-116 and HT-29, and the human prostate cancer cell line PC-3 were cultured in RPMI 1640 medium supplemented with 10% FBS.

Production of RFP Retroviral Vector. For RFP retrovirus production, the *HindIII*/*NotI* fragment from pDsRed2 (Clontech), containing the full-length RFP cDNA, was inserted into the *HindIII*/*NotI* site of pLNCX2 (Clontech) containing the neomycin-resistance gene. PT67, a NIH 3T3-derived packaging cell line (Clontech), expressing the viral envelope, was cultured in DMEM supplemented with 10% FBS. For vector production, PT67 packaging cells, at 70% confluence, were incubated with a precipitated mixture of LipofectAMINE reagent (Life Technologies) and saturating amounts of pLNCX2-DsRed2 plasmid for 18 h. Fresh medium was replenished at this time. The cells were examined by fluorescence microscopy 48 h post-transduction. For selection of a clone producing high amounts of RFP retroviral vector (PT67-DsRed2), the cells were cultured in the presence of 200 to 1,000 μg/mL G418 (Life Technologies) for 7 d. The isolated packaging cell clone was termed PT67-DsRed2 (12–15).

***RFP* Gene Transduction of Cancer Cells.** For *RFP* gene transduction, cancer cells were incubated with a 1:1 precipitated mixture of retroviral supernatants of PT67-DsRed2 cells and RPMI 1640 containing 10% FBS for 72 h. Fresh medium was replenished at this time. Tumor cells were harvested with trypsin/EDTA 72 h post-transduction and subcultured at a ratio of 1:15 into selective medium, which contained 200 μg/mL G418. To select brightly fluorescent cells, the level of G418 was increased up to 800 μg/mL in a stepwise manner. RFP-expressing cancer cells were isolated with cloning cylinders (Bel-Art Products) using trypsin/EDTA. Cells were amplified by conventional culture methods in the absence of selective agent (12–15).

Animal Experiments. Athymic nude mice were kept in a barrier facility under HEPA filtration. Mice were fed with autoclaved laboratory rodent diet (Tecklad LM-485, Western Research Products). All animal studies were conducted in accordance with the principals and procedures outlined in the National Institutes of Health Guide for the Care and Use of Laboratory Animals under assurance A3873–01.

Subcutaneous Tumor Model. Subcutaneous tumors were produced by injection of 3×10^6 noncolored PC-3 or PC-3-RFP human prostate cancer cells in 5-week old nude mice. When tumors reached approximately 6 mm in diameter, the tumors were intratumorally injected with PBS for control or OBP-401 at a dose of 1×10^8 PFU in 100 μL PBS. Mice were examined for fluorescence expression with a long-pass filter (a filter for simultaneous observation of both GFP and RFP) or with specific filters for GFP or RFP.

Peritoneal Carcinomatosis Model of HCT-116 Human Colon Cancer Cells. Five-week-old nude mice were i.p. injected with noncolored HCT-116 or HCT-116-RFP human colon cancer cells (3×10^6 in 200 μL HBSS) using a 27-gauge needle. Twelve days after cancer cell inoculation, mice were injected i.p. with OBP-401 at a dose of 1×10^8 PFU in 200 μL PBS. Five days after virus injection, the abdominal cavity was directly examined by fluorescence imaging under anesthesia.

Pleural Carcinomatosis Model of A549 Human Lung Cancer Cells. Five-week-old nude mice were inoculated with noncolored A549 cells (2×10^6 cells in 200 μL HBSS) into the thoracic space using a 27-gauge needle. Ten days after cancer cell inoculation, OBP-401 at a dose of 1×10^8 PFU in 200 μL PBS was intrapleurally injected. Five days after virus injection, the pleural cavity was directly imaged for GFP expression. GFP-expressing tissues were removed and examined microscopically.

Fluorescence Optical Imaging and Processing. An Olympus OV100 Small Animal Imaging System containing an MT-20 light source was used. High-resolution images were captured directly on a PC (Fujitsu Siemens). Images were analyzed with the use of Cell^R software (Olympus Biosystems) (16).

Histological Examination. For histological studies, GFP-expressing tissues were removed at the time of sacrifice and put into buffered formalin for 24 h at room temperature. All of the tissues were subsequently processed through alcohol dehydration and paraffinization. Tissues were embedded in paraffin and sectioned at 5 μm. All slides were stained by H&E, and examined microscopically.

ACKNOWLEDGMENTS. This project was supported in part by National Cancer Institute Grant CA132242.

1. Sugarbaker PH (2004) Managing the peritoneal surface component of gastrointestinal cancer. Part 1. Patterns of dissemination and treatment options. *Oncology* 18:51–59.
2. Sugarbaker PH (2004) Managing the peritoneal surface component of gastrointestinal cancer. Part 2. Perioperative intraperitoneal chemotherapy. *Oncology* 18:207–219.
3. Glehen O, et al. (2004) Cytoreductive surgery combined with perioperative intraperitoneal chemotherapy for the management of peritoneal carcinomatosis from colorectal cancer: A multi-institutional study. *J Clin Oncol* 22:3284–3292.
4. Kawashima T, et al. (2004) Telomerase-specific replication-selective virotherapy for human cancer. *Clin Cancer Res* 10:285–292.
5. Taki M, et al. (2005) Enhanced oncolysis by a tropism-modified telomerase-specific replication-selective adenoviral agent OBP-405 ('Telomelysin-RGD'). *Oncogene* 24:3130–3140.
6. Umeoka T, et al. (2004) Visualization of intrathoracically disseminated solid tumors in mice with optical imaging by telomerase-specific amplification of a transferred green fluorescent protein gene. *Cancer Res* 64:6259–6265.
7. Kishimoto H, et al. (2006) In vivo imaging of lymph node metastasis with telomerase-specific replication-selective adenovirus. *Nat Med* 12:1213–1219.
8. Fujiwara T, et al. (2006) Enhanced antitumor efficacy of telomerase-selective oncolytic adenoviral agent OBP-401 with docetaxel: Preclinical evaluation of chemovirotherapy. *Int J Cancer* 119:432–440.
9. Sadeghi B, et al. (2000) Peritoneal carcinomatosis from non-gynecologic malignancies: Results of the EVOCAPE 1 multicentric prospective study. *Cancer* 88:358–363.
10. Stepp H, et al. (2007) ALA and malignant glioma: Fluorescence-guided resection and photodynamic treatment. *J Environ Pathol Toxicol Oncol* 26:157–164.
11. Yang M, Luiken G, Baranov E, Hoffman RM (2005) Facile whole-body imaging of internal fluorescent tumors in mice with an LED flashlight. *Biotechniques* 39:170–172.
12. Hoffman RM (2005) The multiple uses of fluorescent proteins to visualize cancer in vivo. *Nat Rev Cancer* 5:796–806.
13. Hoffman RM, Yang M (2006) Subcellular imaging in the live mouse. *Nature Protoc* 1:775–782.
14. Hoffman RM, Yang M (2006) Color-coded fluorescence imaging of tumor-host interactions. *Nature Protoc* 1:928–935.
15. Hoffman RM, Yang M (2006) Whole-body imaging with fluorescent proteins. *Nature Protoc* 1:1429–1438.
16. Yamauchi K, et al. (2006) Development of real-time subcellular dynamic multicolor imaging of cancer-cell trafficking in live mice with a variable-magnification whole-mouse imaging system. *Cancer Res* 66:4208–4214.

A simple biological imaging system for detecting viable human circulating tumor cells

Toru Kojima,[1,2] Yuuri Hashimoto,[1,3] Yuichi Watanabe,[1,3] Shunsuke Kagawa,[1,2] Futoshi Uno,[1,2] Shinji Kuroda,[1,2] Hiroshi Tazawa,[2] Satoru Kyo,[4] Hiroyuki Mizuguchi,[5] Yasuo Urata,[3] Noriaki Tanaka,[1] and Toshiyoshi Fujiwara[1,2]

[1]Division of Surgical Oncology, Department of Surgery, Okayama University Graduate School of Medicine, Dentistry and Pharmaceutical Sciences, Okayama, Japan. [2]Center for Gene and Cell Therapy, Okayama University Hospital, Okayama, Japan. [3]Oncolys BioPharma Inc., Tokyo, Japan. [4]Department of Obstetrics and Gynecology, Kanazawa University School of Medicine, Kanazawa, Japan. [5]Department of Biochemistry and Molecular Biology, Graduate School of Pharmaceutical Sciences, Osaka University, Osaka, Japan.

The presence of circulating tumor cells (CTCs) in the peripheral blood is associated with short survival, making the detection of CTCs clinically useful as a prognostic factor of disease outcome and/or a surrogate marker of treatment response. Recent technical advances in immunocytometric analysis and quantitative real-time PCR have made it possible to detect a few CTCs in the blood; however, there is no sensitive assay to specifically detect viable CTCs. Here, we report what we believe to be a new approach to visually detect live human CTCs among millions of peripheral blood leukocytes, using a telomerase-specific replication-selective adenovirus expressing GFP. First, we constructed a GFP-expressing attenuated adenovirus, in which the telomerase promoter regulates viral replication (OBP-401; TelomeScan). We then used OBP-401 to establish a simple ex vivo method that was able to detect viable human CTCs in the peripheral blood. The detection method involved a 3-step procedure, including the lysis of rbc, the subsequent addition of OBP-401 to the cell pellets, and an automated scan using fluorescence microscopy. OBP-401 infection increased the signal-to-background ratio as a tumor-specific probe, because the fluorescent signal was amplified only in viable, infected human tumor cells, by viral replication. This GFP-expressing virus-based method is remarkably simple and allows precise enumeration of CTCs.

Introduction

Determination of the extent of the disease is the most important factor in predicting the clinical outcome in cancer patients. Primary cancers have been known to shed tumor cells into the blood circulation, which represents the route for systemic tumor cell dissemination (1, 2). Indeed, the presence of circulating tumor cells (CTCs) in the peripheral blood is associated with short survival, and therefore the detection of CTCs is clinically useful as a prognostic factor of disease outcome and/or as a surrogate marker of treatment response (3, 4). Technical advances in immunocytometric analysis and quantitative real-time PCR have made it possible to detect a few CTCs in the blood; however, background expression of cancer-associated antigens, such as cytokeratin 8 (CK-8), CK-18, and CK-19, in normal epithelial cells results in the false-positive detection, and PCR-based methods can not permit analysis of cell morphology. Moreover, there is no sensitive assay for detecting viable CTCs.

The GFP, which was originally identified from the jellyfish *Aequorea victoria*, is an attractive molecular marker for imaging in live tissues because of the relatively noninvasive nature of fluorescent (5–8). It has been reported that hormone-refractory human prostate carcinoma, growing orthotopically in nude mice, efficiently deliver viable tumor cells in the host circulation, which could be detectable using the fluorescence microscopy, when marked by GFP expression (9). In addition, isolated rare CTCs showed an increased metastatic propensity. We reported previously that intratumoral injection of telomerase-specific replication-selective adenovirus expressing the *gfp* gene (OBP-401; TelomeScan) causes viral spread into the regional lymphatics, with subsequent selective replication in neoplastic lesions, resulting in GFP expression in metastatic lymph nodes in *nu/nu* mice (10). The present study extended our previous work, by developing what we believe to be a novel and simple strategy to selectively label human CTCs with fluorescence among millions of peripheral blood leukocytes. The detection method involves 3-steps: the lysis of rbc, the subsequent addition of OBP-401 to the cell pellets, and the automated scan under the fluorescence microscope. This method allows precise enumeration of human CTCs, because OBP-401 can replicate and express GFP fluorescence only in viable tumor cells.

Results

Selective GFP expression in human cancer cells in vitro by OBP-401. OBP-401 (TelomeScan) was constructed by inserting the *gfp* gene under the control of the CMV promoter at the deleted E3 region of the telomerase-specific replication-selective type 5 adenovirus OBP-301 (Telomelysin) (11, 12) (Figure 1). To determine whether telomerase activity is associated with selective GFP expression in different cancer cell lines, we measured human telomerase reverse transcriptase (*hTERT*) mRNA and GFP expression using quantitative real-time RT-PCR analysis and fluorescence microplate reader, respectively. The *hTERT* expression was directly proportional to the fluorescence intensity, and regression analysis confirmed a strong correlation between these numbers ($r^2 > 0.94$) (Figure 1B). H1299 human non–small cell lung cancer cells expressed bright GFP fluorescence as early as 12 hours after OBP-401 infection, and a positive signal for GFP was detected in all cells at 48 hours after infec-

Conflict of interest: Yasuo Urata is an employee of Oncolys BioPharma Inc., the manufacturer of OBP-401 (TelomeScan).

Citation for this article: *J. Clin. Invest.* doi:10.1172/JCI38609.

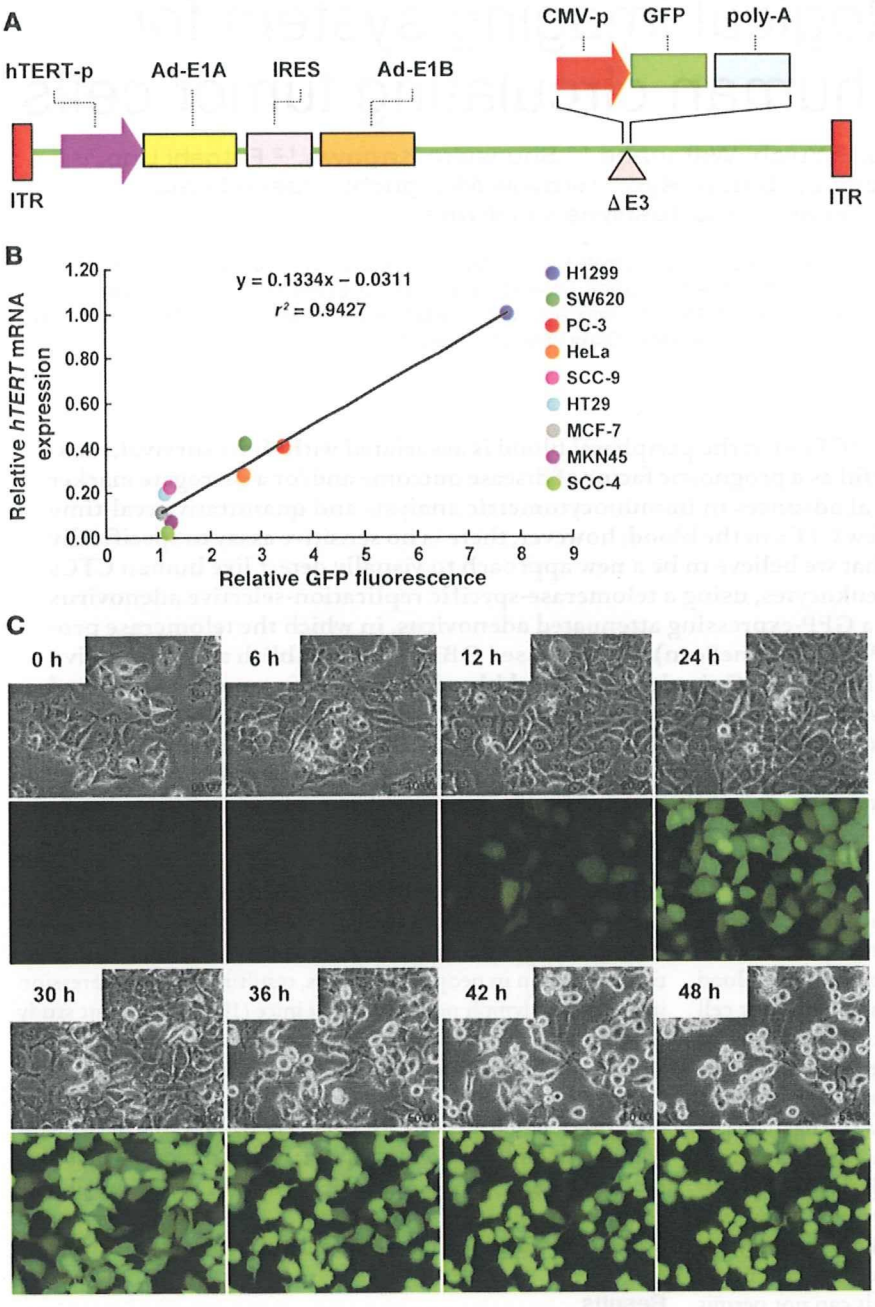

Figure 1
Schematic DNA structure of OBP-401 and selective replication of OBP-401 in human cancer cells. (**A**) OBP-401 is a telomerase-specific replication-competent adenovirus variant, in which the hTERT promoter element drives expression of the *E1A* and *E1B* genes linked with an IRES, and the *gfp* gene is inserted under the CMV promoter into the E3 region for monitoring viral replication. hTERT-p, hTERT promoter; Ad-E1A, adenoviral E1A; Ad-E1B, adenoviral E1B; CMV-p, CMV promoter; poly-A, polyadenylation signal; ITR, inverted terminal repeat. (**B**) Relationship between *hTERT* expression and GFP fluorescence. Relative *hTERT* mRNA expression and GFP fluorescence in human tumor cell lines were determined by real-time RT-PCR analysis and fluorescence microplate reader, respectively. The relative *hTERT* mRNA expression ratios normalized by dividing the value of H1299 cells are presented for each sample. Relative GFP fluorescence was measured 48 hours after OBP-401 infection at an MOI of 10. (**C**) Time-lapse images of H1299 human lung cancer cells were recorded for 48 hours after OBP-401 infection at an MOI of 10. Selected images taken at the indicated time points show cell morphology by phase-contrast microscopy (top panels) and GFP expression under fluorescence microscopy (bottom panels). Original magnification, ×200.

tion (Figure 1C and Supplemental Video 1; supplemental material available online with this article; doi:10.1172/JCI38609DS1). OBP-401 infection also induced GFP expression in other neoplastic cells such as human sarcoma cell lines within 24 hours after infection (Supplemental Figure 1 and Supplemental Video 2). In parallel experiments, OBP-401 infection induced dose-dependent GFP expression in a variety of human cancer cell lines that originated from different organs (Supplemental Figure 2).

Measurement of viable CTCs with OBP-401 in the blood. We used OBP-401 to establish a simple ex vivo method for detecting viable human CTCs in the peripheral blood. As illustrated in Figure 2A, the method involves a 3-step procedure, including the lysis of rbc in 5-ml aliquots of whole blood samples, subsequent addition of 10^4 PFUs of OBP-401 to the cell pellets, and the deposition of cells on polylysine-coated slides, followed by automated scanning under a fluorescence microscope. OBP-401 infection increases the signal-to-background ratio as a tumor-specific probe, because the fluorescent signal can be amplified only in tumor cells by telomerase-specific viral replication. The automated optical scan system provides high speed and accuracy of slide movement in all *x*, *y*, and *z* directions for the acquisition of a large number of high-resolution segmented tile images, at a magnification of ×100 for each tile (Figure 2B). Each optical field is focused automatically before image acquisition. The captured segmented tile images are automatically combined to construct a large image, with a total area of 20 × 20 mm. Since each tile segment can be magnified without the loss of high resolution, OBP-401–infected human tumor cells could be easily visualized with GFP signals in blood smears (Figure

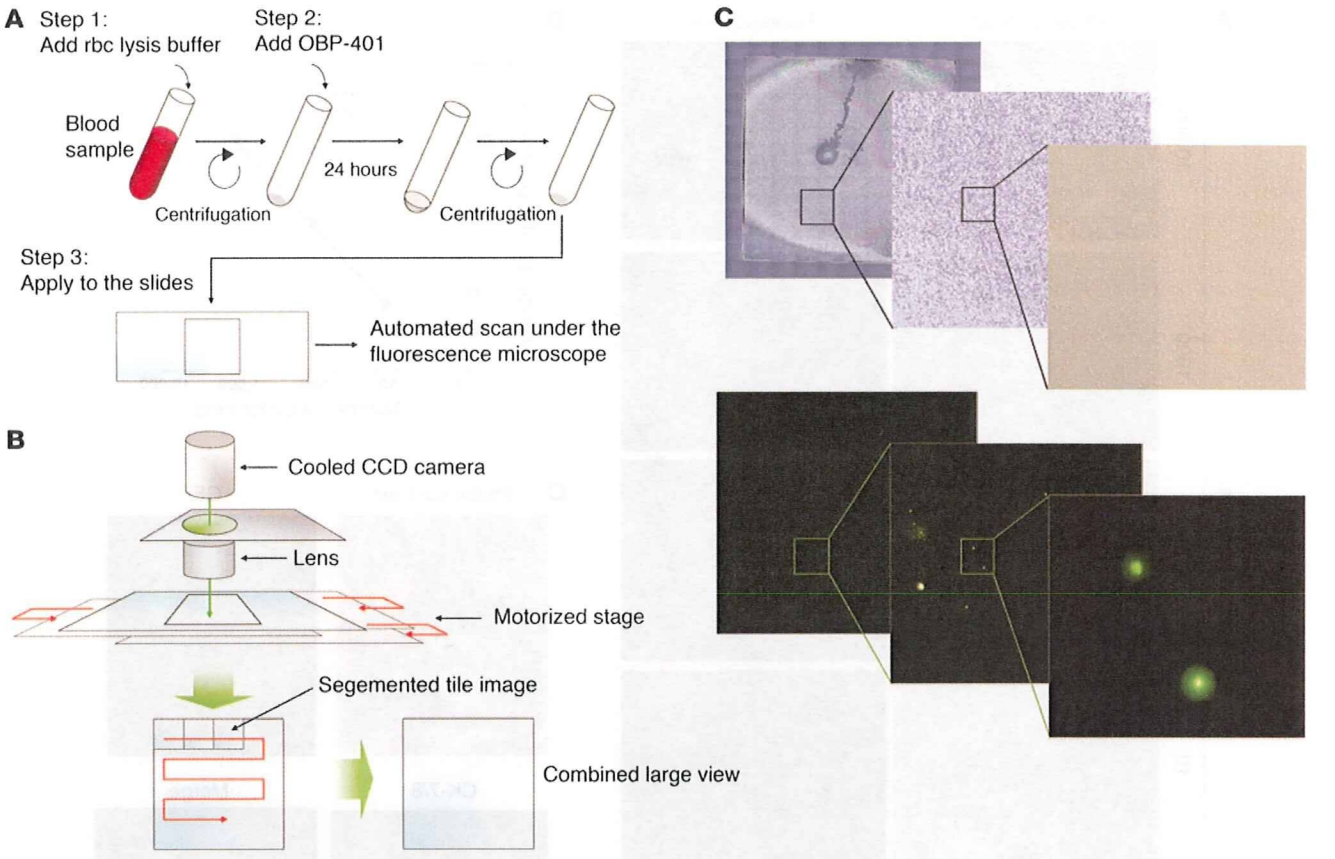

Figure 2

A simple method to detect telomerase-positive cells in the blood. (**A**) Steps in the sample preparation for GFP fluorescence detection. Blood samples (5-ml samples) are collected in heparinized tubes and incubated with rbc lysis buffer containing ammonium chloride (NH_4Cl) for 15 minutes. After centrifugation, cell pellets are mixed with 10^4 PFUs of OBP-401 and incubated at room temperature for another 24 hours. Cells are resuspended in 15 μl of PBS following centrifugation and then placed onto the slide under a coverslip. (**B**) System for automated fluorescence molecular imaging. The automated optical scan system serially captures segmented tile images in the area of the coverslip under fluorescence microscopy. (**C**) A high-resolution large view of the reconstructed tile images. The zoomed image allows easy visualization of GFP-expressing cells among millions of blood leukocytes. Original magnification, ×40 (left panels); ×100 (middle panels); ×400 (right panels).

2C). This automated microscopic scan system allows us to obtain high-magnification images with a large field of view.

Accuracy of CTC detection by ex vivo OBP-401 infection. To test the efficacy and accuracy of the system, whole blood samples from healthy donors were spiked with variable numbers of H1299 human lung cancer cells and then analyzed. Representative images of each sample are shown in Figure 3A. H1299 cells could be distinguished from the other blood cells even at lower magnification. The recovery of tumor cells was consistent over a target frequency range, between 10 and 1,000 cells spiked into 5 ml of blood from normal donors. Regression analysis of the number of GFP-positive cells versus the number of expected tumor cells yielded a correlation coefficient of $r^2 = 0.9996$ (Figure 3B). Thus, the number of GFP-positive cells reflects the actual peripheral blood tumor cell load. We also performed immunohistochemical analysis with anti-human CK-7/8 antibody to ensure that the cells labeled with GFP signals were indeed tumor cells. We used CK-7/8 as a marker for tumor cell detection, as H1299 cells were completely negative for CK-19 (Supplemental Figure 3). The automated microscopic scan system permits repeated scanning of the same fields repeatedly by a 2-dimensional line scanning technology. Merged images of fluorescent detection and CK-7/8 immunostaining confirmed that H1299 human lung cancer cells stably transfected with the *gfp* gene were CK-7/8 positive in the blood smear (Supplemental Figure 3). By using this dual imaging method, we confirmed that the GFP-positive cells were CK-7/8 positive following 24-hour exposure to OBP-401 and were distinguishable from other blood cells (Figure 3C). GFP-expressing cells were also morphologically classified as tumor cells (data not shown).

Comparative analysis of CTC detection by OBP-401, real-time RT-PCR, and flow cytometry. To compare the GFP-based CTC detection and other existing methods, blood samples spiked with variable numbers of H1299 cells were also analyzed. We performed real-time RT-PCR analysis with primers targeting the *hTERT* gene, as OBP-401–mediated GFP expression reflects the telomerase activity (Figure 1B). The number of GFP-positive cells was proportional to the increasing number of H1299 cells, between 10 and 1,000 cells in 5 ml of blood after ex vivo OBP-401 infection (Figure 3B); a significant increase in amplification, however, could not be observed even with 2,000 tumor cells in 1 ml of blood by real-time RT-PCR (Figure 4A), suggesting that the detected *hTERT* mRNA levels might be the background expression. In addition, a

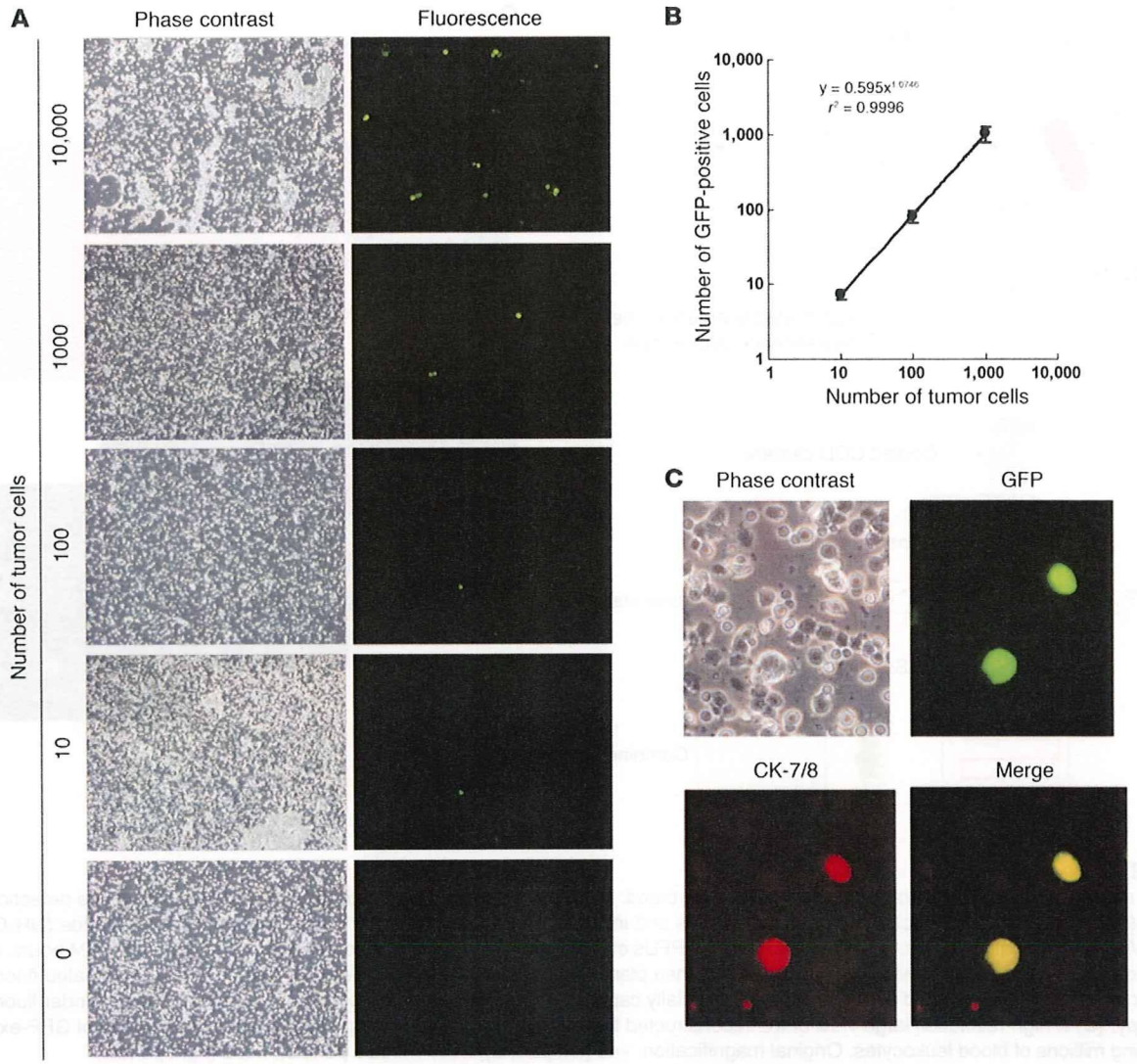

Figure 3
Selective visualization of human cancer cells by OBP-401. (**A**) Phase-contrast and fluorescent images of peripheral blood cells mixed with H1299 human lung cancer cells. Variable numbers of H1299 cells were spiked into 5 ml of whole blood samples from healthy donors and then immediately analyzed for GFP expression. Original magnification, ×100. (**B**) Efficiency of labeling tumor cells added to whole human blood with OBP-401. The number of tumor cells spiked into whole blood versus the number of GFP-expressing cells is plotted. Each value represents the mean ± SD. (**C**) Immunohistochemical staining of GFP-expressing cells for CK-7/8. The blood samples mixed with H1299 cells were analyzed for GFP expression, fixed with 2% glutaraldehyde, and then stained with rhodamine-labeled anti–CK-7/8 antibody. Overlap of green (GFP) and red (CK-7/8) fluorescence was displayed as yellow fluorescence. Original magnification, ×600.

quantitative RT-PCR assay could not detect *CK7* mRNA expression in all samples tested (Figure 4B), although H1299 cells were positive for CK-7/8 (Supplemental Figure 4). We also used flow cytometry to detect H1299 tumor cells in the blood; however, the number of GFP-positive cells following ex vivo OBP-401 infection was much lower than expected (Supplemental Figure 4 and Figure 4C). These results suggest that enrichment of tumor cells or depletion of unwanted cells is necessary for CTC detection by real-time RT-PCR and flow cytometry.

Viable CTCs detected with OBP-401 in patients with various cancers. To examine whether CTCs from cancer patients can be labeled with GFP signals by OBP-401 replication to permit their detection in whole blood, we analyzed fresh blood samples collected from 37 patients with histologically confirmed gastric cancer and 9 patients with other malignancies, including colon cancer, hepatocellular carcinoma (HCC), breast cancer, and non–small cell lung cancer. Although the CTC level varied widely, ranging from 0 to 47 cells in 5-ml samples, 26 gastric cancer patients (70.3%) had more than 1 CTC; there was, however, no apparent relationship between CTC counts and TNM stages (Figure 5A, Table 1, and Supplemental Table 1). CTCs were also identified in samples from 6 of 9 (66.7%) patients with other cancers. The number of CTCs that were isolated ranged from 0 to 56 cells per 5-ml sample (Figure 5B, Table 1, and Supplemental Table 2).

To confirm the infectivity of OBP-401 to tumor cells at the primary sites, we applied this assay to single-cell suspensions isolated

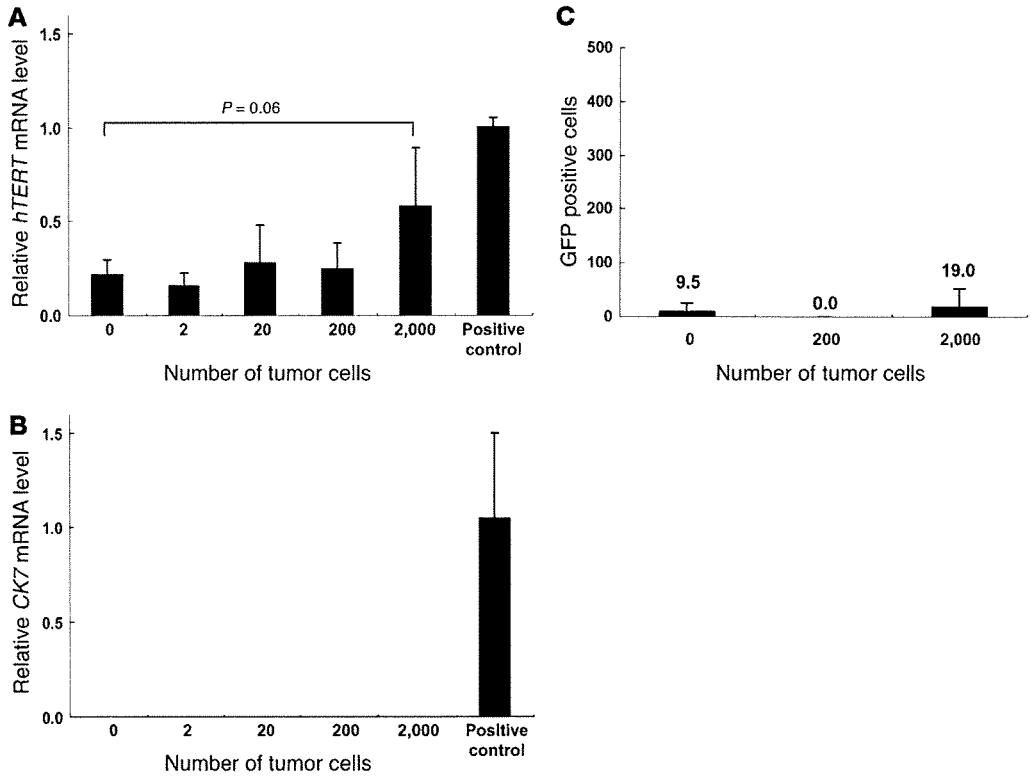

Figure 4

Comparison of the sensitivity of CTC detection by real-time RT-PCR and flow cytometry. (**A** and **B**) Variable numbers of H1299 cells spiked into 1 ml of whole blood samples from healthy donors were prepared. The relative expression of *hTERT* (**A**) and *CK7* (**B**) mRNA was determined by real-time RT-PCR analysis. The amount of *hTERT* and *CK7* mRNA was normalized with data from the real-time amplification of the *GAPDH* housekeeping gene. The blood without H1299 cells was used as a negative control, and H1299 cells without the blood were used as a positive control. (**C**) Flow-cytometric enumeration of variable numbers of H1299 cells mixed in 1 ml of blood samples. After the lysis of rbc, blood samples were infected with 10^4 PFUs of OBP-401 for 24 hours, and then subjected to flow-cytometric analysis. The numbers above the bars indicate the actual numbers of GFP-positive cells. Each value represents the mean ± SD of triplicate experiments.

from surgically removed primary tumors. A gallery of cellular images showed sufficient GFP expression in tumor cells obtained from gastric and colon cancer patients, following OBP-401 infection at a MOI of 100 (Figure 6). The size and morphology of GFP-labeled cells isolated from primary tumors were consistent with those of CTCs detected in the peripheral blood of the same patients.

We further assessed the CTC dynamics in patients who were undergoing chemotherapy or surgery, to demonstrate the clinical potential of our approach for monitoring treatment responses. The results from a representative patient with advanced stage IV gastric cancer (case 1) are shown in Figure 7A. A 5-ml blood sample contained 6 CTCs before treatment. Fourteen days after the initiation of systemic chemotherapy, 7 CTCs were detected in the peripheral blood; the patient, however, had no CTCs after 2 cycles of chemotherapy. A patient who had a recurrence of gastric cancer in the regional lymph nodes (case 10) had decreased CTC counts after a cycle of chemotherapy (Figure 7B). Elimination or reduction of CTCs correlated well with a decrease in the levels of tumor markers such as CEA, CA19-9, and CA125. In contrast, the number of CTCs gradually increased in an advanced gastric cancer patient (case 25) who developed retroperitoneal tumor invasion despite chemotherapy (data not shown). As this patient showed no elevated levels of tumor markers, the kinetic of CTC numbers would enable a faster prediction of the treatment response than that of other radiographic imaging methods. In the 4 patients who underwent surgery (gastric cancer, cases 5 and 9; colon cancer, cases 3 and 4), the CTC level dropped 4 weeks after complete resection (Figure 7, C and D). These results suggest that enumeration of CTCs might be useful for monitoring the efficacy of local and systemic treatments.

Discussion

Early and accurate evaluation of therapeutic efficacy is the hallmark of successful cancer treatment. We have described a simple method, without any complicated processing steps, for detecting viable human CTCs in the peripheral blood, by using telomerase-specific GFP-expressing adenovirus. Viable CTCs may be a less-invasive, repeatable biomarker for monitoring tumor responses against various types of therapies, although its clinical significance is still debatable. In our pilot study, reported herein, serial blood sampling demonstrated that surgical removal of primary tumors was associated with decreased CTC counts. Thus, quantitative detection of CTCs can be also a substantial surrogate marker for treatment efficacy in candidates for chemotherapy.

The technical platform of CTC enumeration has improved rapidly (13). PCR-based techniques, which are commonly used to detect CTCs (14, 15), can detect dead tumor cells and cell-free circulating DNA or RNA, which may result in overestimation of the neoplastic